NUREG/CR-6420

Self-Monitoring Surveillance System for Prestressing Tendons

Phase I Small Business Innovation Research

Manuscript Completed: November 1995
Date Published: December 1995

Prepared by
H. Tabatabai

Construction Technology Laboratories, Inc.
5420 Old Orchard Road
Skokie, IL 60077

H. L. Graves, NRC Project Manager

Prepared for
Division of Engineering Technology
Office of Nuclear Regulatory Research
U.S. Nuclear Regulatory Commission
Washington, DC 20555-0001
NRC Job Code W6475

Abstract

Assured safety and operational reliability of post-tensioned concrete components of nuclear power plants are of great significance to the public, electric utilities, and regulatory agencies. Prestressing tendons provide principal reinforcement for containment and other structures. In this phase of the research effort, the feasibility of developing a passive surveillance system for identification of ruptures in tendon wires was evaluated and verified. The concept offers high potential for greatly increasing effectiveness of presently-utilized periodic tendon condition surveillance programs.

A one-tenth scale ring model of the Palo Verde nuclear containment structure was built inside the Structural Laboratory. Dynamic scaling (similitude) relationships were used to relate measured sensor responses recorded during controlled wire breakages to the expected prototype containment tendon response. Strong and recognizable signatures were detected by the accelerometers used. It was concluded that the unbonded prestressing tendons provide an excellent path for transmission of stress waves resulting from wire breaks.

Accelerometers placed directly on the bearing plates at the ends of tendons recorded high-intensity waveforms. Accelerometers placed elsewhere on concrete surfaces of the containment model revealed substantial attenuation and reduced intensities of captured waveforms. Locations of wire breaks could be determined accurately through measurement of differences in arrival times of the signal at the sensors. Pattern recognition systems to be utilized in conjunction with the proposed concept will provide a basis for an integrated and automated tool for identification of wire breaks.

Contents

List of Tables

List of Figures

List of Figures (cont'd.)

List of Figures (cont'd.)

SELF-MONITORING SURVEILLANCE SYSTEM FOR PRESTRESSING TENDONS

1.0 INTRODUCTION

1.1 Background

Considering the 40-year operating license term for existing U.S. nuclear facilities, the majority of plants are approaching the re-licensing decision. Reliability of plant structures will be a crucial parameter in the decision. Therefore, acute understanding of extent of structural aging is of utmost safety and economic importance.

Many containment structures for nuclear power plants have, as their main structural elements, large numbers of unbonded prestressing tendons. Many nuclear power plant auxiliary structures have also been constructed of prestressed concrete with unbonded tendons. These tendons generally consist of cold drawn steel wire or strand inside ducts filled with grease. The steel elements are highly stressed. Tendons provide the principal reinforcement for gravity, seismic, projectile and internal pressurization loading conditions, and as such are extremely crucial elements of the plant structure.

In unbonded tendons, there exists no bond between strands or wires and the surrounding concrete. Major stress changes in wires occur only after the force (prestress) in the tendon is overcome due to overloading.

Because of the criticality of reliable tendon function, periodic tendon monitoring programs are required for containment and other post-tensioned nuclear structures in the United States. These tests include selective, limited inspections, residual prestress force monitoring tests, tendon property tests, and inspection/testing of filler grease. Therefore, anchorage assembly hardware are inspected, stress levels of selected tendons are checked using the lift-off method, and small samples of prestressing steel (surveillance tendons) are removed for testing and examination for corrosion or other conditions.

Although the above surveillance methodology appears well founded, intervals between tendon surveillance activities are oftentimes longer than desirable and these operations are costly. Therefore, introduction of non-invasive continuous monitoring efforts may be prudent to gather data in preparation for re-licensing application. This need may become more acute when tendon deterioration mechanisms (including corrosion) accelerate with age. It is important to note that some deterioration phenomena may remain undetected even by tendon lift-off tests at loads less than nominal tendon capacity. To our knowledge, there exist no reliable methods for continuous comprehensive sensor-based monitoring of wire breaks in the tendons.

In 1991, CTL began to experiment with crude single channel wire fatigue cracking detection systems for a laboratory acceptance testing fixture for bridge stay cables. These cables, similar to containment tendons in size and configuration, are comprised of parallel strands encased in a

polyethylene or steel pipe. Strands were epoxy-coated or bare, depending on the cable design. Most stay cables were grouted with cementitious materials. Although the length of stay cables on bridges can be as large as several hundred feet, the test cable lengths range between 15 and 20 feet. Testing of these cables incorporates two million cycles of fatigue loading followed by static proof loading to 95% of nominal strength. The acceptance requirements are: (1) not more than 2% of wires can break during fatigue testing, and (2) the cable must sustain the target static load after undergoing the fatigue test.

Since the acceptance criterion for wire breakage pertains only to those occurring during fatigue testing, a wire break detection system was devised to estimate how many and when wire breaks occur during fatigue testing. As highly-stressed stranded wires break, they generate stress waves that travel along the tendon to the anchorages.

CTL attached an accelerometer at one cable anchorage to monitor shock waves due to wire breaks. A computer continuously monitors the output of the accelerometer at high speed and captures (records) the event if the output exceeds a preset threshold. Each recorded event is evaluated with respect to shape and intensity to see whether it is due to wire rupture or other conditions.

To date, a total of eighteen stay cable acceptance tests have been performed by CTL. In a great majority of those, the detection system was utilized during fatigue and static tests. Good correlation was found between predicted and actual number of wire breaks especially when wire break signatures of a cable of similar design were available for comparison. The stay cable test specimens, however, are shorter and less complex installations than containment tendons. They are grouted instead of greased, and are generally oriented in straight alignment instead of curved alignment.

Based on the experience with wire rupture monitoring in short cables, it was envisioned that a multi-sensor system with self-monitoring features could be developed to continuously and automatically "listen" for potential wire ruptures in prestressing tendon groups.

Since the ultimate result of deterioration of prestressing tendons will be the loss of steel section or individual wire ruptures, such a detection system will enable utilities and/or regulatory agencies to monitor and assess the effects of aging on prestressing tendons. This system, in conjunction with periodic in-service inspections, can be used to correlate strand conditions with wire breaks, perhaps lessening future reliance on invasive, costly tendon surveillance programs. The frequency of detected wire breaks will also identify wire deterioration rates.

1.2 Anticipated Results

Phase I research was designed to evaluate the feasibility of the proposed concept for containment tendons and lay the foundation for work in Phase II. The anticipated results of this proposed approach, if carried over into subsequent phases, are as follows:

- A system will be developed that will continuously monitor, detect and record wire break data in unbonded tendons of nuclear containment and other post-tensioned structures.
- The developed system will include sensor systems, data acquisition hardware and data analysis software.
- This system, in combination with inspections, will allow a better and more thorough assessment of aging effects on the condition of crucial prestressing tendons. This capability will, in turn, provide another tool for decisions regarding re-licensing of nuclear power plants or other operational factors.
- This system will also be useful as a maintenance tool. If locally severe corrosion conditions lead to pitting and wire rupture, then those conditions can be identified and corrected.

- This system will permit monitoring of wire breaks during full scale in-situ containment structural integrity tests.

1.3 Technical Objectives and Scope

The general objective of Phase I research was as follows:

- To evaluate feasibility of a self-monitoring electronic sensor system for use in automated identification and characterization of containment prestressing wire rupture in service.

Specific objectives of Phase I research were as follows:

- To evaluate whether wire ruptures in containment tendons resulting from deterioration (corrosion or other factors) produce recognizable repeatable shock waves or acoustic signatures that can be reliably detected and accurately interpreted. Specifically, issues related to type of tendons (greased) and curvature of tendons were to be addressed.
- To evaluate the candidate sensor types for consideration.
- To evaluate potential data capture and analysis techniques including the computer hardware and software necessary to maximize automation of process for detection and evaluation of sensor outputs.

Questions that needed to be addressed in Phase I were as follows:

- Does this concept have realistic, practical potential for its stated objective?
- What are the candidate systems for sensors and capture and analysis of sensor outputs in a power plant environment?

This phase I research work was conducted within the scope of the following five tasks.

- Task 1 - Literature Search
- Task 2 - Laboratory Test Plan
- Task 3 - Laboratory Testing
- Task 4 - Review of Waveform Analysis Options
- Task 5 - Report

2.0 PHASE I RESEARCH PROGRAM

2.1 Literature Search

A review of literature in the following areas was performed:

- Detection of breaks in wires, strands, cables, and chains
- Detection of transients and shock waves (limited)
- Scaling laws, modelling, and similitude in dynamics of structures (limited)

- Similitude in acoustics (limited)
- Signal processing, neural networks (limited)

In the area of break detection, papers directly related to wire break detection in tendons of nuclear containment walls were not found. However, a number of papers were found on acoustic monitoring of wire breaks in wire ropes and also in prestressed concrete pipes.

The Bureau of Reclamation of the U.S. Department of the Interior has issued a report detailing development of an acoustic method for detection and identification of wire break locations in prestressed concrete pipelines.[1] These wires are wrapped around large-diameter (21 ft diameter) prestressed concrete pipes and are used as primary reinforcement for the structure. Wire breaks have, on a number of occasions, resulted in catastrophic failure of such pipes.

Hydrophones were used in the Bureau study since attenuation of acoustic signals in water is significantly less than in concrete (around 1 dB per 1000 yards). Hydrophones were placed 1000 ft apart. Field tests were performed to develop and refine the procedures. It is interesting to note that although wire breaks were readily recognizable audibly, the response spectra did not show prominent distinguishing characteristics. Therefore, an advanced signal processing system was developed utilizing a neural network classifier to identify breaks. The data base of identified breaks were then used to further train the net.

Research in the Netherlands on acoustic inspection and monitoring of prestressing tendons and bars in offshore concrete structures was presented in a report in 1989.[2] This report discussed experiments on prestressing strands strung in air between two posts, on concrete test beams, and on concrete bridges. The beams were apparently bonded prestressed concrete. Fracture energy was noted to propagate mainly through concrete and to a lesser degree through the strand. The report concluded that detection ranges will be limited because of leakage of acoustic signals from the prestressing cables into the surrounding concrete. It is interesting to note, however, that these researchers saw potential for this technology on containment vessels as shown in the following paragraph:

"Because of the limitations on the detection range, which can be even further reduced by mechanical noise, the methods described in this report cannot be recommended for general use in prestressed concrete structures. There are, however, special cases, such as for instance ***containment vessels***, where acoustic inspection and monitoring deserves further attention."[2] It is believed that the Dutch researchers may have been referring to the expected low signal attenuation rates in unbonded (greased) tendons of containment vessels.

A number of papers were published by researchers at the University College in Cardiff, United Kingdom on detection of wire breaks in wire ropes[3,4,5,6,7,8]. Tests on relatively short lengths of 12 mm and 40 mm diameter wire ropes were performed under rising load and fatigue loading conditions. In general, good agreement was reported between recorded events and the actual number of broken wires. It was also reported that background noise is distinguishable and wire breaks can be detected over relatively long lengths of rope. However, there were problems in detection when multiple fractures occurred on the same wire.

These researchers suggested that waveforms from wire breaks inside a rope have longer duration and lower amplitudes when compared to breaks of individual wires. They also concluded that determination of location of break using arrival times of waveform at two sensors (linear source measurements) is reasonably accurate.

Laura, Vanderveldt, and Gaffney[9] presented experimental results on detection of wire rope failure by means of monitoring stress emissions in the cable system. An accelerometer was attached to the cable and the rope specimens were subjected to an increasing load until failure.

The following conclusions were made:

- Acoustic detection methods appear feasible to warn against impending failure.
- The number and amplitude of emissions increase with increasing load.
- The type of stress wave emissions depends on cable material and construction,

Harris and Dunegan [10] performed acoustic emission testing of wire rope under tensile and fatigue loading conditions. They reported that emissions began at about half the maximum load, and ample warning of impending strand failure was obtained. A one-to-one correlation was obtained between the number of broken wires and the number of events observed at 40 db gain. They concluded that acoustic emission techniques are well suited for studies of failure mechanics and nondestructive evaluation of wire ropes.[10]

Acoustic emission monitoring of wire ropes used to lift counterweights on a lift span bridge in California was reported by Harris.[11] A number of 2-in. diameter, 180-ft long cables were instrumented with acoustic sensors and monitored. An overall gain of 80 db, and bandpass of 100-300 kHz were used. Measurements of attenuation along the cable were in the range of 1 to 5 db/in. Considerable emissions were observed from two cables. Harris concluded that the acoustic emission techniques were capable of giving early warning of impending failures.[11]

Kobe Steel in Japan has been developing a method for detection of wire breaks in HiAm sockets of stay cables for bridges.[12] These cables incorporate parallel wires. This procedure is a simple send-receive ultrasonic method. An ultrasonic probe is attached to the wire end and a wave is transmitted. If there is a wire breakage, the ultrasonic wave is reflected as an echo at the break point. From the delay time of the echo, the presence and position of the wire breakage can be measured. However, researchers reported that the attenuation constant in a wire constrained by cast material is much larger than that in a free wire and decreases as frequency increases, in contrast to a free wire. The acceptable distance for detection of breaks depends on the cable structure, especially on cast materials. For HiAm sockets this distance is reported to be 0.5 m.

Based on the review of literature available on the topic of detection of wire breaks, it appears that the proposed methodology for detection of wire breaks in unbonded tendons of containment walls is supported by successful development of similar technologies in other areas.

In the area of shock and transient detection, a number of papers were identified. These papers presented various transient detection algorithms. A number of papers addressed neural-network-based methods for detection and classification of transients.

Since a scale-model test of a containment wall is proposed in this study, a limited search of literature on the subject of similitude and scaling laws in vibrations of concrete structures was performed.[13,14,15] The scaling relationships presented in Section 2.2.2 of this report (Table 1) were found to be appropriate for use in this project.

A limited search of literature in the areas related to scaling laws and acoustic emissions was performed. One paper referred to small-scale acoustic monitoring of corrosion fatigue crack growth in offshore steel.[16] However, that research did not utilize a small-scale (geometrically scaled) model of the structure, but rather used small steel specimens. Two books written by Murphy[17] and Olson[18] briefly discuss the basic scaling relationships for acoustical systems. Murphy discusses relevant acoustical parameters such as intensity, acoustical resistance, etc., and presents basic scaling relations.

Limited search and review of literature in the area of signal processing was also performed. Commercially-available systems and software were found that could be adapted for use in development of a recognition system for this specific application.

2.2 Test Methodology and Details

2.2.1 General

Based on the results of the literature search, a review of the original test plan was carried out, and the following test methodology was deployed.

To evaluate the feasibility of the proposed concept, an assessment of possible shapes, frequencies and intensities of the waveforms generated by the sensor is required to ascertain whether they are detectable under various conditions. However, considering the massive size of typical containment structures, it was not feasible to test the concept at a large scale in Phase I research. Therefore, it was proposed that a series of tests be performed on a one-tenth scale ring model of a containment structure in the CTL Structural Laboratory. The choice of a geometric scale of 10 was based on space and economic limitations and resulted in the largest size model that could be built and tested within those limitations. To relate the results of tests on the model to the prototype response, it is necessary that the model be a true representation of the prototype based on the laws of similitude.

2.2.2 Scaling Relationships

Tabatabai et al[19] presented scaling (similitude) relationships for blast effects on structures. Table 1 presents scaling relationships for some of the parameters involved. These scaling laws were used for small-scale (1/60 to 1/80) model testing of underground protective structures subjected to conventional blast loading in a research project sponsored by the U.S. Air Force. These same relations can also be used to relate model and prototype responses in the tests reported here.

Since materials used for the model and prototype i.e. concrete, prestressing wire, grease, etc. are the same (or very similar), then material property requirements listed in Table 1 are satisfied. These include parameters such as modulus of elasticity, material wave speed, Poisson's ratio, density, etc.

Achieving an ideal or "true" model is not entirely possible in a great majority of cases. Some degree of distortion is generally present. The potential impact of such distortions must be considered and evaluated in the design of such models. For example, Table 1 shows that acceleration in the model should be n times the acceleration in the prototype. Theoretically, this same requirement should apply to the acceleration due to gravity. However, the model tests are conducted at 1g (the same as prototype). This introduces a distortion in the model. The effect of this distortion in the model, however, would be an incorrect modeling of gravity (dead load) stresses which are believed to have an insignificant effect for the purposes of this study.

One factor that is significant and must be properly considered is the amount of energy released from a single wire break in a strand. According to scaling laws, the wire (strand) energy in the model should be related to the prototype wire (strand) energy based on the following relationship (see Table 1):

$$E_{nm} = (1/n^3)\, E_{np} \qquad (1)$$

where

E_{nm} = Stored elastic energy of the strand in the model

E_{np} = Stored elastic energy of the strand in the prototype

n = Scale factor (10 in this case)

If diameter of wires (strands) in the model were 1/10 the diameter of the prototype wires (strands) and they were both (model and prototype) tensioned to the same stress level, then the requirements of the above equation would be satisfied and a distortion of model in this regard would not be introduced. However, the prototype strands are typically 0.5 or 0.6 in. in diameter, and the diameter of strands in the model are 0.25 in. Therefore, the model wire diameter is only approximately one-half of the prototype instead of one-tenth. This introduces a significant distortion which must be considered.

Considering that the 1/4-in. diameter strand is the smallest prestressing strand commercially available, the most appropriate way to address this issue was considered to be a reduction in the tensile stress of the wire so that the proper amount of elastic energy is stored in the wire. Therefore, based on the following equations, the amount of stress (tensioning force) in the model wire was reduced to achieve a correct value for E_{nm}.

Stored elastic energy in wire or strand can be related to the force applied and the resulting displacements as follows:

$$E_{nm} = 1/2\ F_m\ \Delta_m$$

and

$$E_{np} = 1/2\ F_p\ \Delta_p$$

where F_m and F_p are tension forces in the model and prototype strands, respectively, and Δ_m and Δ_p are displacements due to applied forces in the model and prototype strands, respectively.

However,

$$\Delta_m = (F_m\ L_m) / (A_m\ E_m)$$

and

$$\Delta_p = (F_p\ L_p) / (A_p\ E_p)$$

where parameters L, A, and E denote total length, cross sectional area, and modulus of elasticity of strand, respectively. Subscripts m and p refer to model and prototype, respectively.

The following relationships can written using information in Table 1:

$$L_p = n\ L_m$$

$$E_p = E_m$$

Equation 2 can be written after substituting the above parameters into Equation 1.

$$F_m = (F_p/n)\ (A_m/A_p)^{0.5} \qquad (2)$$

For a 1/2 in.-diameter prototype strand, the typical initial tension force (F_p) of 30,980 lbs corresponds to a stress of 0.75 percent of Guaranteed Ultimate Tensile Strength (GUTS). The cross sectional area of 1/2 in. strand is 0.153 $in.^2$, and GUTS is 270 ksi. The ratio of strand cross sectional areas in the model and prototype is approximately 0.25. Therefore,

$F_m \approx 1.55$ kips

As discussed in Section 2.2.3, this force has to be increased to account for live end strand seating losses.

The amount and details of mild reinforcement in the model were also different from the properly-scaled reinforcement in the prototype structure and therefore introduce distortions in a true model. However wave transmissions are believed not to be significantly affected because the stress waves will mainly travel along the unbonded prestressing strands to the anchorages.

Also, in a true model, stresses due to prestressing in the model and prototype concretes should be the same. However, the amount of prestress in the model concrete is in fact far less than the prototype. Again, this distortion is considered insignificant in this case. The magnitude of stress in concrete is not believed to have a major influence on stress wave transmissions through concrete. Also, the primary path for stress wave transmission is through unbonded strand and not concrete.

Finally, 1/4-in. thick steel liner plates are used in the prototype on the inside of the containment structure. However, scaled liners were not used in the model as they are believed to be insignificant with regard to the purposes of this study due to the reasons given above.

2.2.3 Description of Model

A small-scale ring model of a containment structure was built inside the CTL Structural Laboratory. The prototype structure used for this model was the Palo Verde Nuclear Generating Station. A dimensional scale of 10 was used. Therefore, the 150-ft diameter cylinder and 4-ft thick wall of the prototype were modelled with a 15-ft diameter ring and a 4 3/4-in. thick wall.

Dimensions of the structure are shown in Figure 1. Three buttresses (14 in. by 4 in.) built approximately 120 degrees apart provided anchorages for strands. A general view of the completed ring model is shown in Figure 2.

The mild reinforcing steel consisted of No. 3 bars @ 12 in. on each face of concrete in both vertical and horizontal directions with additional reinforcement provided in the buttresses. Longitudinal steel consisted of curved (circumferential) bars. Figure 3 shows reinforcement details.

Prestressing strands used were the smallest size strands that are commercially available. They were 1/4 in.-diameter, 250 ksi seven-wire prestressing strands. Each individual strand was greased and placed inside a polyethylene (PE) tube with an inside diameter of 3/8 in. and an outside diameter of 1/2 in. Post-tensioning grease was donated by a major post-tensioning contractor (Dywidag Systems International, Inc.). The tubes containing strands were then placed inside the forms and attached to the reinforcing bars as shown in Figures 4 and 5.

Strands were tensioned using a small hydraulic jack and a calibrated pressure cell. Two sets of strand chucks with wedges (live and dead ends) were used to grip the strands at each end. A 0.5 in. thick steel bearing plate was placed under each chuck bearing on the buttress. Based on an assumed live end wedge seating of 3/16 in., the tensioning force was increased from 1.55 to 2.0 kips to compensate for wedge seating losses.

A number of pockets (2" x 3" openings) were built into the wall to allow cutting of wires during tests (Figures 4 and 6). Some openings were located near anchorages while others were located

near the mid-length of strand. This was done to compare the intensity and shape of waveforms at various distances from the wire break. Also, this allowed an evaluation of the effectiveness of predicted wire break locations.

The concrete used had a specified 28-day compressive strength of 5000 psi. It had a maximum aggregate size of 3/8 in. (pea gravel). Superplastisizer was used to achieve a slump of 5 in.

2.2.4 Sensors and Monitoring System

Two accelerometers attached to the structure at various positions were used for the tests. Accelerometers were PCB Model 337D04. According to the manufacturer, these sensors have a mounted resonant frequency greater than 12 kHz, a voltage sensitivity of approximately 100 mV/g, a range of ± 50 g, and a resolution of 0.002 g.

At least one of the accelerometers was placed on the live (stressing) end anchorage (on the steel bearing plate) while the other accelerometer was placed on either the concrete surface or the dead end anchorage. Figure 7 shows an accelerometer placed on live end bearing plate. Selected individual wires in the seven-wire strand were cut with a small grinding device as shown in Figure 8.

A 4-channel Tektronix Model TDS 420A digital storage oscilloscope (DSO) was used to acquire data from the sensors. The digitizing rate was set at one million samples per second and a total of 15,000 points were acquired per channel for each trigger. The system was set to display 10 percent (1.5 ms) pre-trigger information. This DSO has a built-in disk drive that stores waveforms in spreadsheet format. It also performs Fast Fourier Transforms (FFT) and other mathematical operations. The FFT options utilizes the first 10,000 points of the waveform.

These features prompted selection of this DSO over the previously proposed dynamic analyzer which had far slower digitizing rates. The higher digitizing speed is considered important for accurately determining differences in arrival times at the two sensors for prediction of wire break locations.

2.3 Laboratory Testing

2.3.1 Test Details

A total of eighteen wire break tests were performed on four strands. Table 2 summarizes the tests performed. Figures 9 and 10 show details of each test including locations of accelerometers and distances from wire break locations to the ends of strand. The threshold voltages selected in different tests were based on the desire to capture the actual rupture of the wire and not the lower level stress waves generated by the cutting process.

2.3.2 Test Results

Figures 11 through 45 show time and frequency domain responses for the eighteen tests conducted. Only 1.5 ms pre-trigger and 8 ms post-trigger information are shown in the time response figures. All graphs show measured responses of the model (not prototype). It should be noted that, based on scaling relationships shown in Table 1, the output (in volts or g's) of an accelerometer placed at a corresponding (similar) position on the prototype would be smaller by a factor of 10 (n = 10).

For example, if the wire cut location were 20 ft from a buttress in the model, then a wire cut at the corresponding location on the prototype (200 ft from same buttress) would register acceleration values equivalent to one-tenth of the model output. The time scale, on the other hand, would have to be multiplied by 10 to obtain corresponding times on the prototype. The frequency scale should be divided by ten.

$a_p = a_m / 10$

$t_p = 10\ t_m$

$f_p = f_m / 10$

In the above equations, a, t, and f refer to acceleration, dynamic time, and signal frequency, respectively. Prototype and model are identified with subscripts p and m, respectively.

Test Nos. 1 through 3 were conducted on Strand No. 1. Accelerometer No. 1 (A1) was placed at the live (stressing) end anchorage while Accelerometer No. 2 (A2) was located at the dead end (Figure 9). The wire cut location was 16-1/2 in. away from strand mid-length. The difference in distance from the cut point to both sensors was therefore 33 in.

Figures 11 through 16 show time and frequency domain responses for the three tests performed on Strand No. 1. It is clearly evident that A1 registered strong responses (up to 3 volts or 30 g's) for a duration of 2 to 3 ms. However, A2 response was much weaker (approx. 0.7 volts or 7 g's) with the same duration as A1. It is not clear why sensor amplitudes were so much different. However, it is possible that a kink or bend may have been present in the strand between the cut point and A2 which resulted in additional attenuation of signal.

It is clearly evident that the arrival times of the waveform at the two sensors are different due to the longer time it takes for the signal to travel the extra distance of 33 in. to A2 when compared to A1. This measured time difference is approximately 0.16 ms. The predicted time of arrival difference can be calculated using the theoretical longitudinal wave speed in the steel wire.

Longitudinal wave velocity for thin rods (steel wire) can be determined from the following equation:[20]

$$C_l = (E/\rho)^{0.5} \qquad (3)$$

where

C_l = longitudinal wave velocity

E = Young's modulus of elasticity

ρ = density of material

For a prestressing wire with a modulus of elasticity of 30,000,000 psi and a unit weight of 490 lbs/ft^3:

$C_l \approx 16{,}850$ ft/sec

A velocity of 16,850 ft/sec will result in a time difference of 0.163 ms for a distance of 33 in. which is very close to the measured value. Therefore, it is clear that prediction of wire break locations is feasible and can be accurate if sufficiently high digitizing rates are utilized in capturing waveforms.

The frequency domain responses for the first three tests indicate that the frequency content is less than 20 to 30 kHz. Knowledge of the frequency range of the signal will help in the selection of appropriate sensors for further development of the system. Also, if the frequency spectra for all tests were to exhibit prominent and repeatable distinguishing characteristics, then they would be useful as detection tools. The noticeable peak at approximately 14 kHz may be due to the mounted

resonant frequency of the accelerometer used. The FFT response of A1 in Test No. 1 was accidentally deleted from DSO memory and is therefore not shown in Figure 12.

Figures 17 and 18 show time and frequency domain responses for the first wire cut test (Test No. 4) performed on Strand No. 2. A1 was placed at the live end anchorage while A2 was at the dead end. Location of wire cut was very close to A1. Therefore, it is clear that A1 registered a much higher amplitude response than A2. The difference in arrival times of the waveform at the two sensors is very noticeable because of a 27 ft-7 in. difference in distances between the cut point and the two sensors. This measured time of arrival difference is approximately 1.65 ms. The predicted time of arrival difference based on the theoretical longitudinal wave speed is 1.64 ms. Again, the frequency content of the signal is less than 20 kHz.

Figures 19 through 28 show time and frequency responses in Test Nos. 5 through 9 on Strand No. 2. A1 and A2 were placed at the live and dead end anchorages, respectively. The difference in distances between the cut point and the two sensors was 27 ft-7 in. These tests are different from Test No. 4 in that the location of wire cut was close to A2 instead of A1. As expected, the output of A2 was much stronger than A1. Test No. 9, in which the center or king wire was cut, shows higher intensity and signal duration than the other four similar tests. Frequency content of the A2 signal in these tests was up to 40-60 kHz.

Test Nos. 10 through 14 were performed on Strand No. 3. They were the first tests in which one accelerometer was placed on the concrete surface instead of the bearing plates at the ends of strand. A1 was placed on the live end anchorage while A2 was placed on the buttress concrete surface 6 in. above A1. The wire cut was near mid-length of the strand. Figures 29 through 38 show time and frequency responses in these tests. As expected, A2 produced consistently weaker signals when compared to A1. This is due to the attenuation of the signal traveling through concrete.

In the last series of tests (Test Nos. 15 through 18) on Strand No. 4, A1 was located on the live end anchorage while A2 was placed on the concrete wall's outside surface directly over the strand, and at a distance of 2 ft from the cut point. Figures 39 through 46 show time and frequency responses of the sensors in these tests. It is clear that the sensor output on the concrete surface (A2) is not as strong as the sensor output on the bearing plate (A1). In Test No. 18, an attempt was made to cut the last four wires in Strand No. 4 simultaneously. This resulted in a much stronger output for A1 when compared to the other three tests.

2.3.3 Test Result Summary

Duration of signals in various model tests are within 3 to 6 ms. This translates into durations of 30 to 60 ms in the prototype structure. Signals recorded at close proximity to the wire breaks display longer durations.

The amplitude of signals (from model tests) ranged from a few g's to over 50 g's. The prototype amplitudes would therefore range from a fraction of 1 g to over 5 g's. In general, the amplitude of signal is related to proximity to wire break location. However, there were cases (such as tests on Strand No. 1) where the amplitudes at one location were less than expected. This may have been due to possible obstructions in the path of the strand.

The predominant signal frequency contents are within 20-30 kHz. This translates into prototype frequencies of 2-3 kHz. It is clear that the shape of the frequency spectra in various tests are different and therefore may not be directly used as a wire break detection tool. Researchers at the Bureau of Reclamation who studied detection of wire breaks in pipelines reached a similar conclusion.[1] They developed a neural network based detection system for their application.

2.4 Options for Sensors and Signal Processing

Tests reported above were performed using common piezoelectric accelerometers. Other researchers have used acoustic sensors to detect cracking, microfractures, corrosion activity, etc. at signal frequencies above 100 kHz. However, high-frequency components of the acoustic signal attenuate rapidly over relatively short distances.[21] Since these sensors need to monitor wire rupture events at long distances, it is believed that the common accelerometer may be the most appropriate sensor for further development of this concept. It is clearly evident from the tests that accelerometers produce sufficiently strong responses at cable ends to be detected (even at the prototype level). Since a relatively large number of sensors would be required for the actual containment structures, it may be appropriate to utilize more economical semi-conductor type accelerometers for this field application. The accelerometers to be used in the development of the system should have a range of at least $\pm$10 g's, with a frequency response of up to at least 10 kHz. Special attention should be paid to noise suppression in the system.

The digitizing rate for recording of the sensor outputs has to be high enough to allow a determination of the location of wire breaks based on differences in arrival times. For example, a digitizing rate of 100 kHz for two sensors with identical time base of reference, can theoretically provide an accuracy of 2 in.

Regarding signal processing options, it is believed that a method based on neural network algorithms may provide the most appropriate choice. Complete pattern recognition software packages are commercially available that include statistical and neural network solutions.

3.0 PHASE I SUMMARY

In this Phase I research effort, the feasibility of a self-monitoring surveillance system for detection of wire ruptures in prestressing tendons of nuclear containment and other structures was established. The system offers high potential of increasing effectiveness of presently-utilized periodic localized inspections with continuous global monitoring systems.

Therefore, it was proposed that a multi-sensor monitoring system be developed that will continuously 'listen' for events i.e. wire breaks. The system will then identify a captured event as a wire break and determine its location.

Testing of this concept at the scale of an actual containment structure was not considered necessary or economically feasible in the Phase I research project. Therefore, to verify its feasibility, a one-tenth scale model of the Palo Verde Nuclear Generating Station secondary containment was built inside the CTL Structural Laboratory. The ring model had a diameter of 15 ft, a wall thickness of 4 3/4 in., and a height of 6 ft. Small-diameter prestressing strands encased in polyethylene ducts filled with grease were embedded in the wall. Two accelerometers were placed at various locations specially on bearing plates for the test strands. Wires were cut at different locations and the sensor outputs were recorded with a digital storage oscilloscope. Scaling (similitude) relationships were used to relate the model responses to the prototype.

Based on the results of the Phase I research program, the concept was judged feasible. It possesses a realistic and practical potential for successful development.

4.0 PHASE I CONCLUSIONS

Based on an evaluation of the results of tests on a small-scale model of a nuclear containment structure, the following can be concluded:

1. Development of a passive surveillance system for detection of wire breaks in unbonded tendons of containment or other structures is feasible.

2. The output of sensors indicates that wire breaks produce strong recognizable signatures that can be detected in the prototype structure. Unbonded tendons (strands or wires inside grease-filled ducts) provide an excellent transmission path for stress waves resulting from a wire break.

3. Locations of wire breaks can be accurately determined by determining differences in arrival times of the signal at the two sensors (located at cable anchorages) using the longitudinal wave speed in steel wires. A high-speed scanning system is required to allow determination of wire break locations using differences in arrival times of the signal.

4. Sensors placed on the tendon bearing plates generated strong outputs as a result of wire breaks. However, accelerometers placed on concrete surfaces produce recognizable but weaker responses because of attenuation of signal strength in passage through concrete.

5. An evaluation of sensor types to be used in development of this proposed concept indicated that the most appropriate sensor is an accelerometer with a frequency range of up to at least 10 kHz with a minimum range of $\pm$ 10 g's.

6. The frequency spectra of captured wire break events did not produce repeatable distinguishing characteristics in various types of tests. Therefore, they may not be useful as the only tool in detection of wire breaks. Pattern recognition systems containing neural network algorithms are recommended for development of an automated detection system.

5.0 RECOMMENDATIONS FOR FUTURE WORK

It is recommended that additional work be performed to further develop and refine the proposed concept. This additional work will build on the results of Phase I research to design, build, and test a prototype detection system for containment and other unbonded post-tensioned structures. Specifically, the following issues need to be further studied and addressed:

- Additional tests on the one-tenth scale ring model to develop a data base of wire break signatures for training of a neural network. This work will also involve introduction of false events in addition to real wire breaks. Attention will be given to a global monitoring of responses of a number of sensors throughout the structure to single events.

- Design and selection of various hardware and software components of the automated detection system including sensors, wiring, scanning systems, data storage systems, data analysis hardware including a central computer, pattern recognition software, wire break locator software, and remote monitoring and warning systems. Attention will be paid to the ruggedness and long-term performance of the system.

- Design of the optimum sensor placement schemes for various applications.

- Development of a prototype detection system composed of all the hardware and software components

- Testing of this system on the small-scale model in addition to an actual containment structure.

6.0 REFERENCES

1. Travers, F., "Acoustic monitoring of Prestressed Concrete Pipe at the Agua Fria River Siphon," Report No. R-94-17, U.S. Department of the Interior, Bureau of Reclamation, Denver, Colorado, December, 1994, 30 pp.

2. DeSitter, W.R. (Chairman), "Acoustic Inspection and Monitoring of Prestressing Tendons and Bars, "CUR-VB Committee B30 Report No. 124, Centre for Civil Engineering Research, Codes and Specifications for Concrete, Gouda, Netherlands, 1989, 31 pp.

3. Casey, N.F., and Taylor, J.L., "The Evaluation of Wire Ropes by Acoustic Emission Techniques," British Journal of NDT, November, 1985, pp. 351-356.

4. Casey, N.F., Holford, K.M., and Taylor, J.L., "The Acoustic Evaluation of Wire Ropes Immersed in Water," NDT International, Vol. 20, No. 3, June, 1987, p 173-176.

5. Casey, N.F., and Taylor, J.L., "An Instrument for the Evaluation of Wire Ropes: A Progress Report," British Journal of NDT, Vol. 29, No. 1, January 1987, pp. 18-21.

6. Casey, N.F., Holford, K.M., and Taylor, J.L., "Wire Break Detection During the Tensile Fatigue Testing of 40 mm Diameter Wire Rope," British Journal of NDT, Vol. 30, No. 5, September 1988, pp. 338-341.

7. Casey, N.F., Wedlake, D., Taylor, J.L., and Holford, K.M., "Acoustic Detection of Wire Rope Failure," Wire Industry, Vol. 52, No. 617, May 1985, pp. 307-309.

8. Wedlake, D., White, H., Holford, K.M., and Taylor, J.L., "Acoustic Energy in Wire Failure," Wire Industry, Vol. 54, No. 646, October 1987, pp. 628-629.

9. Laura, P.A., Vanderveldt, H.H., and Gaffney, P.G., "Mechanical Behavior of Stranded Wire Rope," MTS Journal, Vol. 4, No. 3, May-June 1970, pp. 19-32.

10. Harris, D.O., and Dunegan, H.L., "Acoustic Emission Testing of Wire Rope," Materials Evaluation, Vol. 32, No. 1.

11. Harris, D.O., "Acoustic Emission Monitoring of Lift Span Cables on Dumbarton Bridge," Dunegan/Endevco Technical Memorandum DC-72-TM11, Report for the Department of Public Works, Division of Bay Toll Crossings, State of California, December, 1972., 11 pp.

12. Suzuki, N., Takamatsu, H., Kawashima, S., Sugii, K., and Iwasaki, M., "Ultrasonic Detection Method for Wire Breakage," Kobelco Technology Review, No. 4, August 1988, pp. 23-26.

13. Farrar C.R., Baker, W.E., and Dove, R.C., "Dynamic Parameter Similitude for Concrete Models," ACI Structural Journal, American Concrete Institute, Vol. 91, No. 1, January-February 1994, pp. 90-99.

14. Krawinkler, H., and Moncarz, P.D., "Similitude Requirements for Dynamic Models," ACI SP73-1, H.G. Harris, Editor, American Concrete Institute, 1982.

15. Caccese, V., and Harris, H.G., "Earthquake Simulation Testing of Small-Scale Reinforced Concrete Structures," ACI Structural Journal, American Concrete Institute, Vol. 87, No. 1, January-February 1990, pp. 72-80.

16. Thaulow, C., and Berge, T., "Acoustic Emission Monitoring of Corrosion Fatigue Crack Growth in Offshore Steel," NDT International, Vol. 17, No. 3, June 1984, pp. 147-153.

17. Murphy, G., Similitude in Engineering, The Ronald Press Company, New York, 1950, 302 pp.

18. Olson, H.F., Acoustical Engineering, D. Van Nostrand Co., Princeton, New Jersey, 1957.

19. Tabatabai, H., Bloomquist, D., McVay, M.C., Gill, J.J., and Townsend, F.C., "Centrifugal Modeling of Underground Structures Subjected to Blast Loading," Report No. AFESC/ESL-TR-87-62, Air Force Engineering Services Center (now Air Force Civil Engineering Support Agency), Tyndall Air Force Base, Panama City, Florida, March 1988, 319 pp.

20. Bray, D.E., and McBride, D. (Editors), Nondestructive Testing Techniques, Part 4, John Wiley & Sons, Inc., New York, 1992, 765 pp.

21. Hardy, H.R., "Applications of Acoustic Emission Techniques to Rock and Rock Structures: A State-of-the-Art Review," Acoustic Emissions in Geotechnical Engineering Practice, Drnevich and Gray (editors), American Society for Testing and Materials, 1981, 209 pp.

ACKNOWLEDGEMENTS

The author wishes to express his appreciation to the NRC and Mr. Herman Graves for their support of this research effort.

The author also expresses his appreciation to the following CTL staff: Mr. Adrian T. Ciolko who was instrumental in the initial development of the concept and provided review and oversight of the project; Mr. Timothy J. Dickson (formerly of CTL) for his assistance in the project; Messrs. Greg Neiweem, Brad Anderson, and Felix Gonzales for their efforts in building the test specimen; Mr. Ralph Reichenbach for his preparation of graphs and drawings; and Ms. Nancy Adams for typing this report.

Dywidag Systems International of Bolingbrook, Illinois donated grease for unbonded tendons. Their support is greatly appreciated.

Table 1. Dynamic scaling relationships.

Parameter	Symbol	Scaling Relationship
Stress	σ	$\sigma_m = \sigma_p$
Dimension or Length	L	$L_m = L_p/n$
Displacement	d	$d_m = d_p/n$
Acceleration	a	$a_m = n\, a_p$
Velocity	v	$v_m = v_p$
Pressure	P_o	$P_{om} = P_{op}$
Energy	E_n	$E_{nm} = E_{np}/n^3$
Dimension	D	$D_m = D_p/n$
Density	ρ	$\rho_m = \rho_p$
Material Modulus	E	$E_m = E_p$
Material Strength	F	$F_m = F_p$
Material Wave Speed	C	$C_m = C_p$
Area	A	$A_m = A_p/n^2$
Volume	V	$V_p = V_p/n^3$
Mass	M	$M_m = M_p/n^3$
Strain	ε	$\varepsilon_m = \varepsilon_p$
Dynamic Time	t	$t_m = t_p/n$
Signal Frequency	f	$f_m = n\, f_p$
Poisson's Ratio	μ	$\mu_m = \mu_p$
Force	E_f	$F_{fm} = F_{fp}/n^2$

m = model

p = prototype

n = length scale

Table 2. Wire break test summary.

Test No.	Strand No.	Wire Cut Opening Identification*	Trigger Threshold (mV) and Slope
1	1	1M-B	+ 360, Positive
2	1	1M-B	+ 360, Positive
3	1	1M-B	+ 360, Positive
4	2	2E-A	+ 520, Positive
5	2	2E-B	+ 920, Positive
6	2	2E-B	+ 920, Positive
7	2	2E-B	+ 920, Positive
8	2	2E-B	+ 920, Positive
9	2	2E-B	+ 920, Positive
10	3	3M-A	+ 520, Positive
11	3	3M-A	+ 520, Positive
12	3	3M-A	+ 520, Positive
13	3	3M-A	+ 520, Positive
14	3	3M-A	+ 520, Positive
15	4	4E-C	+ 920, Positive
16	4	4E-C	+ 920, Positive
17	4	4E-C	+ 920, Positive
18	4	4E-C	+ 920, Positive

* See Figure 4 for locations of openings

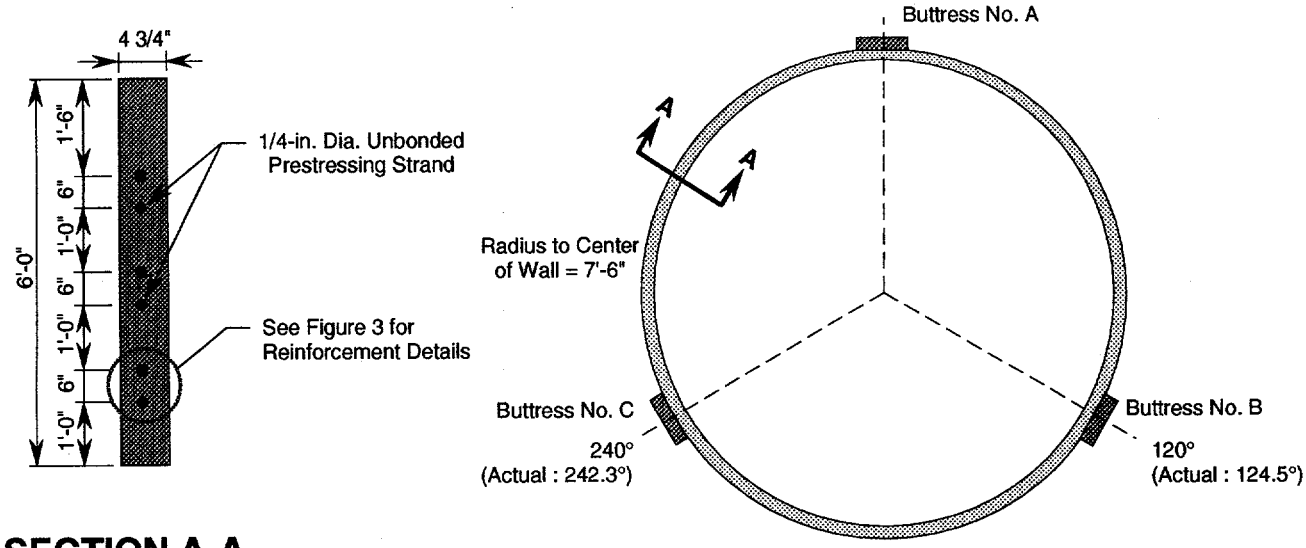

SECTION A-A

PLAN OF CONTAINMENT MODEL

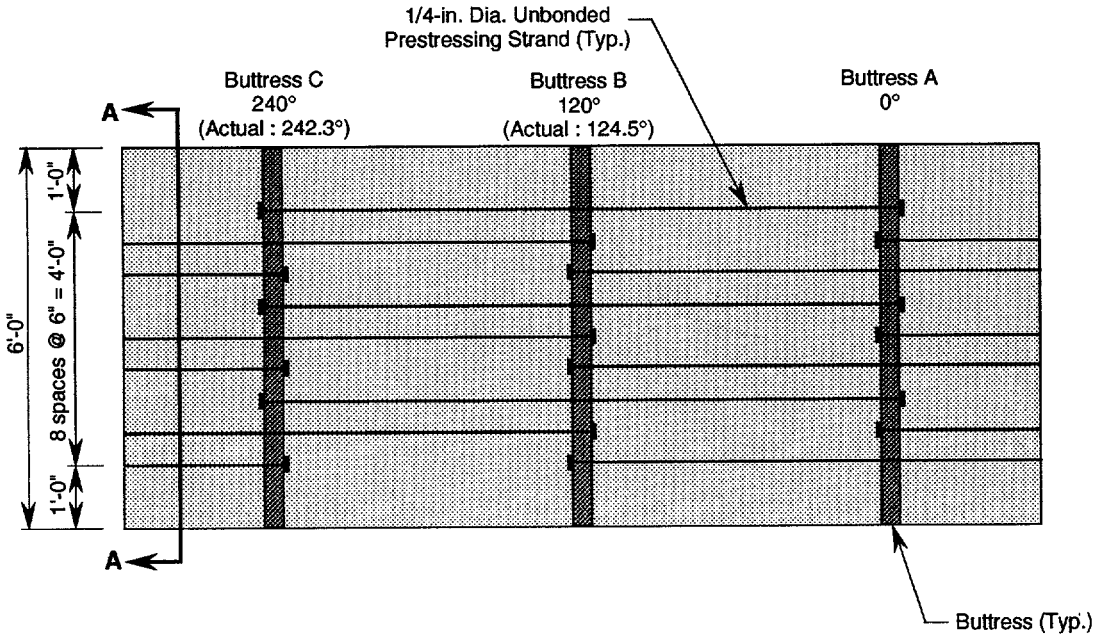

ELEVATION
HORIZONTAL WALL TENDONS

Figure 1. One-tenth scale ring model of containment structure.

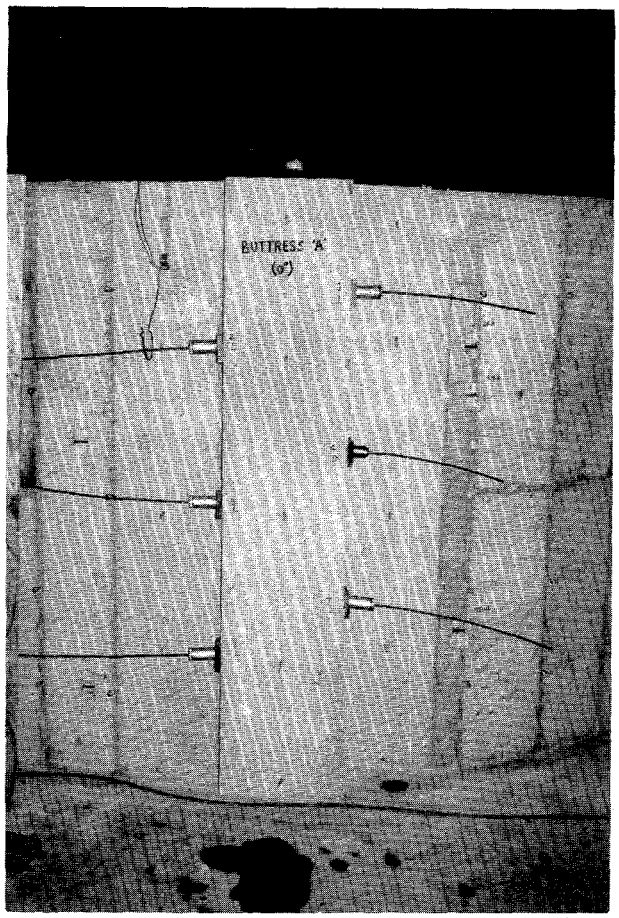

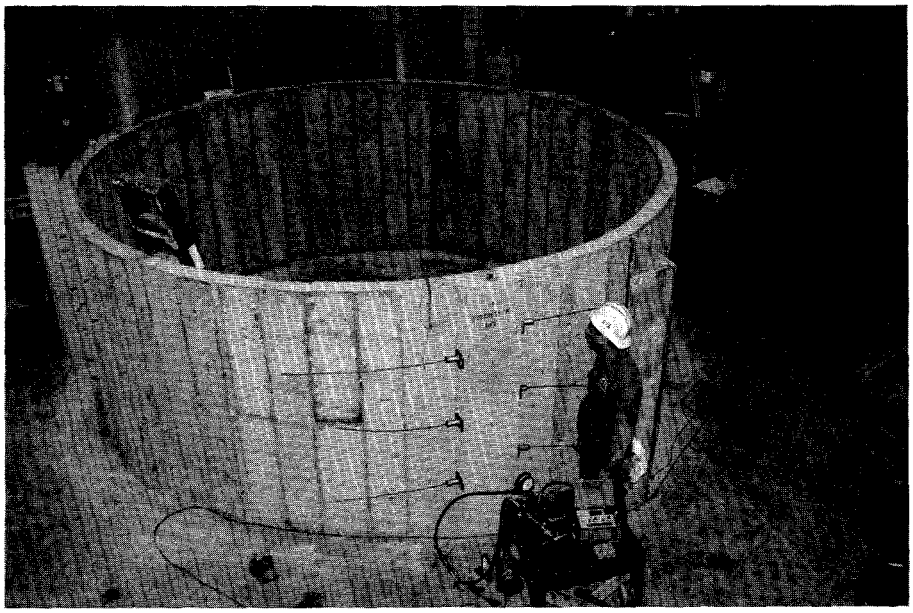

Figure 2. General view of constructed ring model.

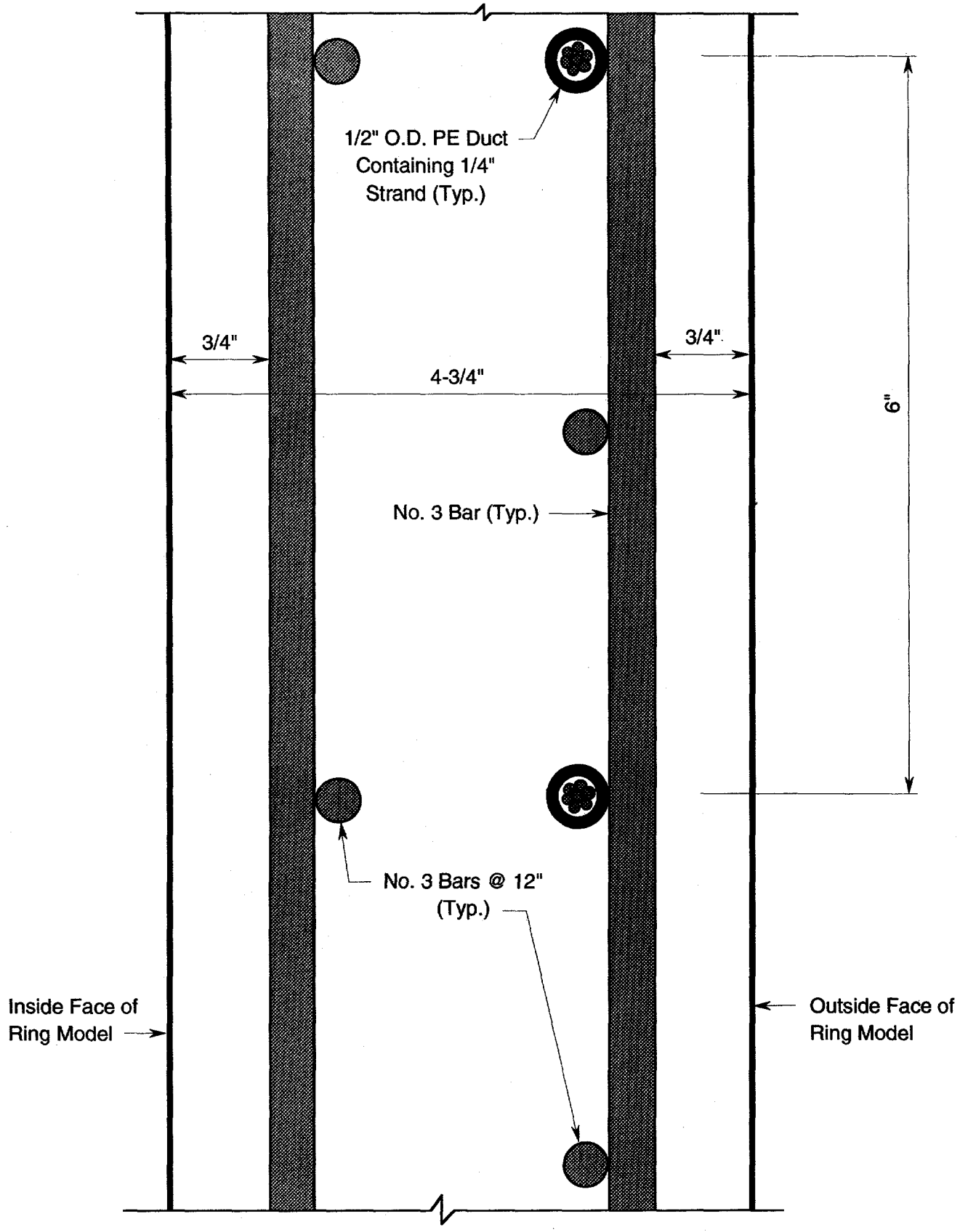

Figure 3. Reinforcement details.

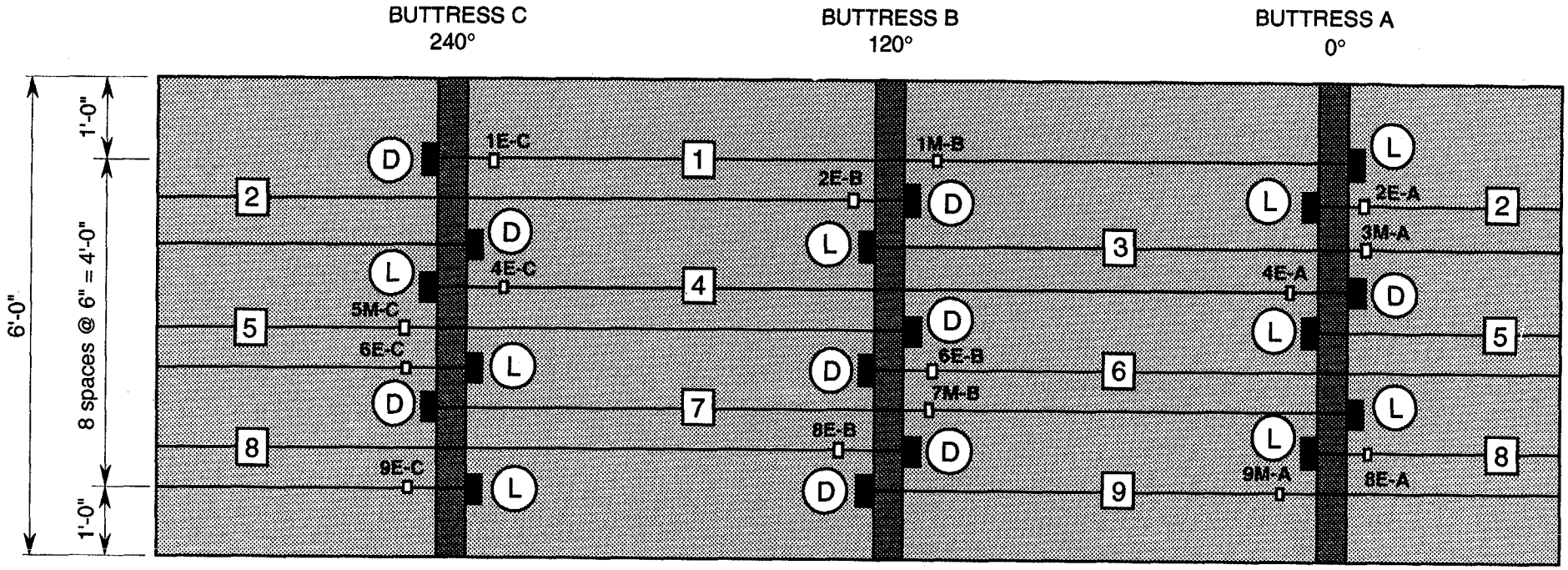

ELEVATION

Bearing Plate (1/2") & Chuck

3" X 2" blockout (Styrofoam) to the Strand Level to Allow cutting of Wires

Strand No

Dead (D) or Live (L) Ends

Figure 4. Locations of tendons and openings.

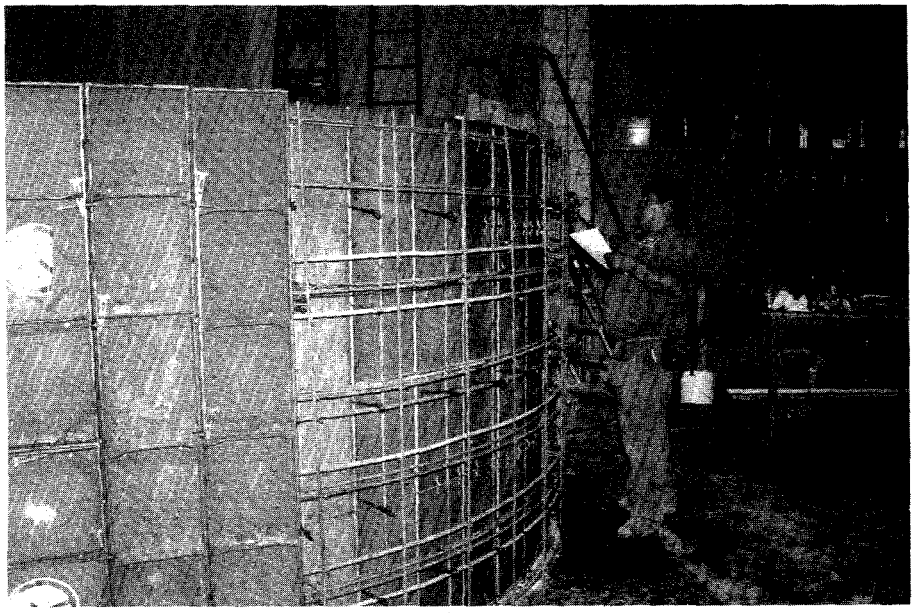

Figure 5. Strands and bars placed inside the form.

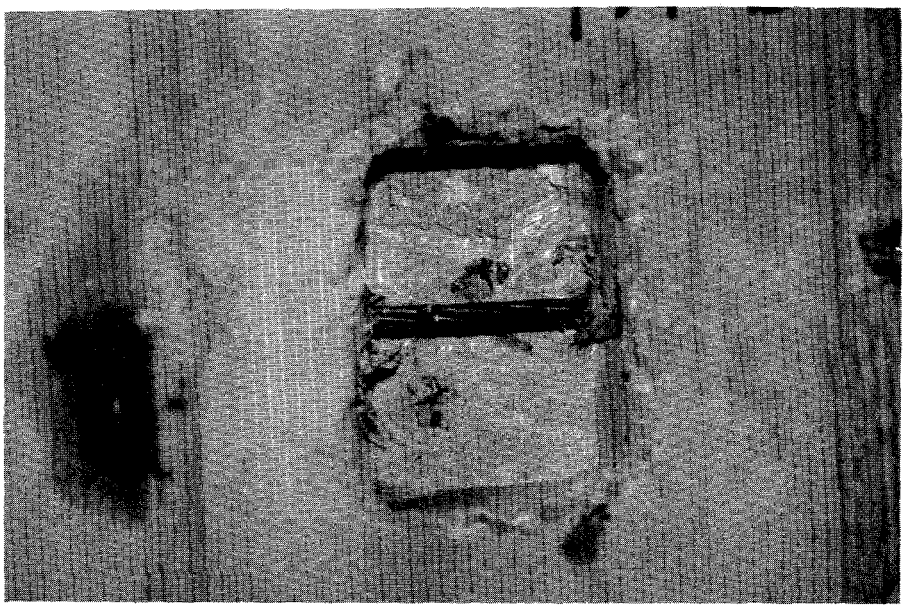

Figure 6. Typical opening in the wall to access strand for cutting.

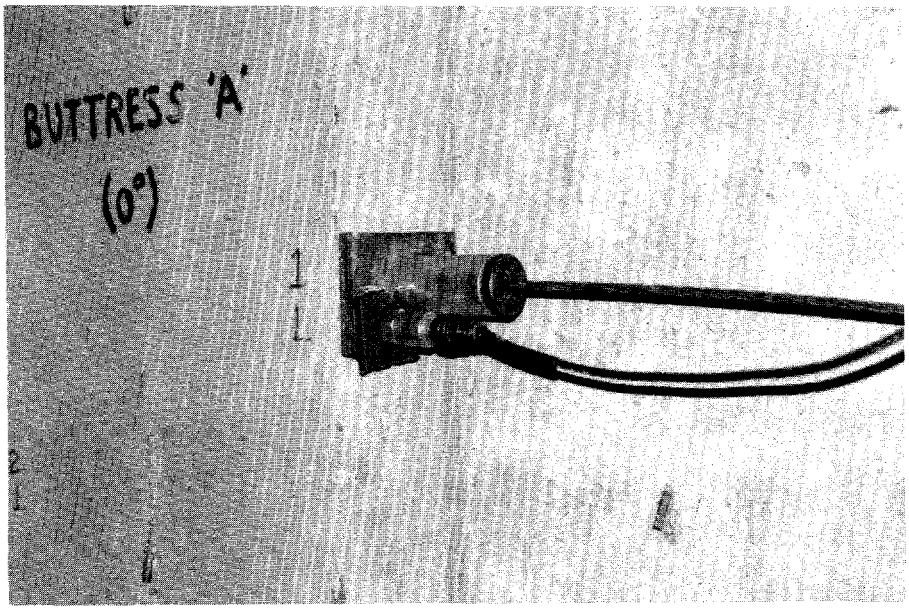

Figure 7. Accelerometer attached next to anchorage.

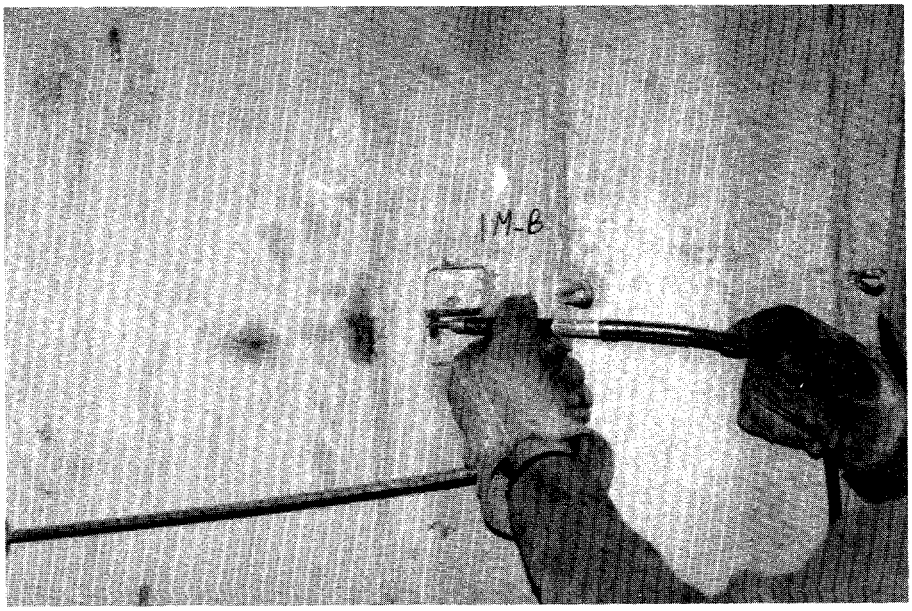

Figure 8. Cutting of wires with small grinder.

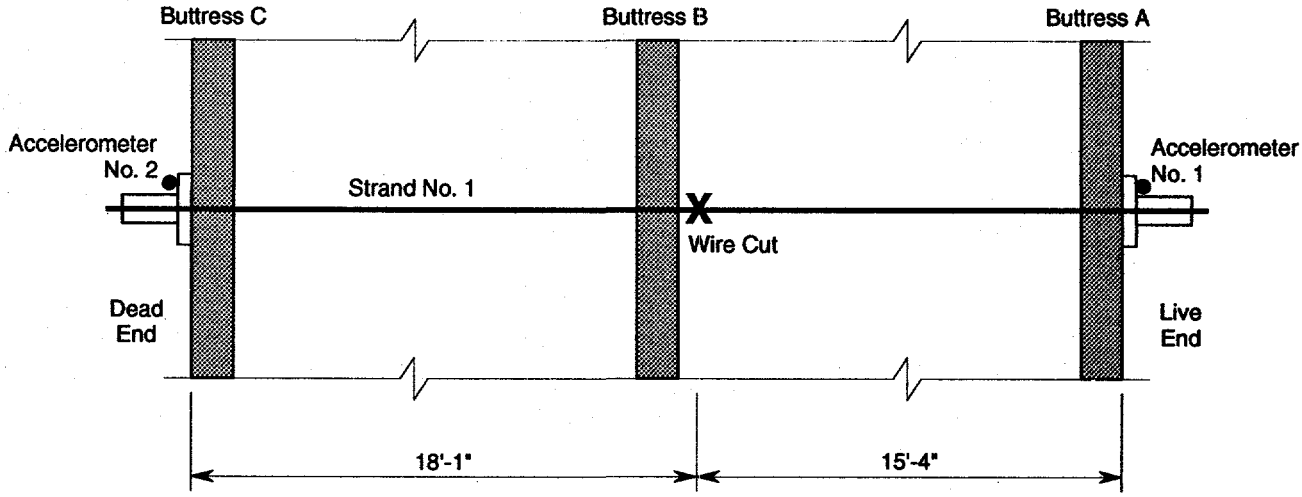

Accelerometer and Wire Cut Locations for Test No.'s 1, 2 and 3

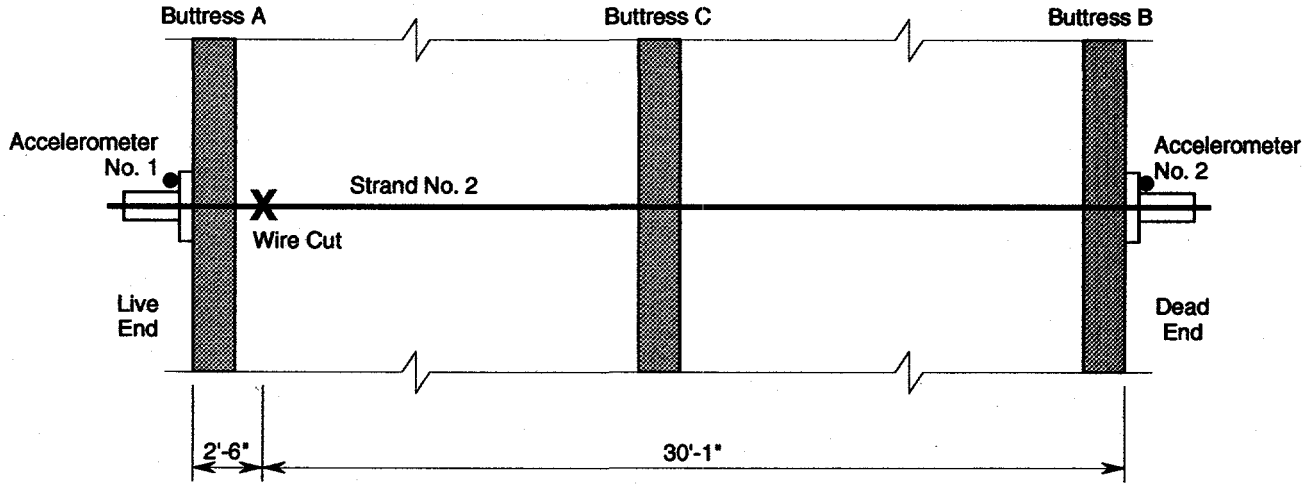

Accelerometer and Wire Cut Locations for Test No.'s 4

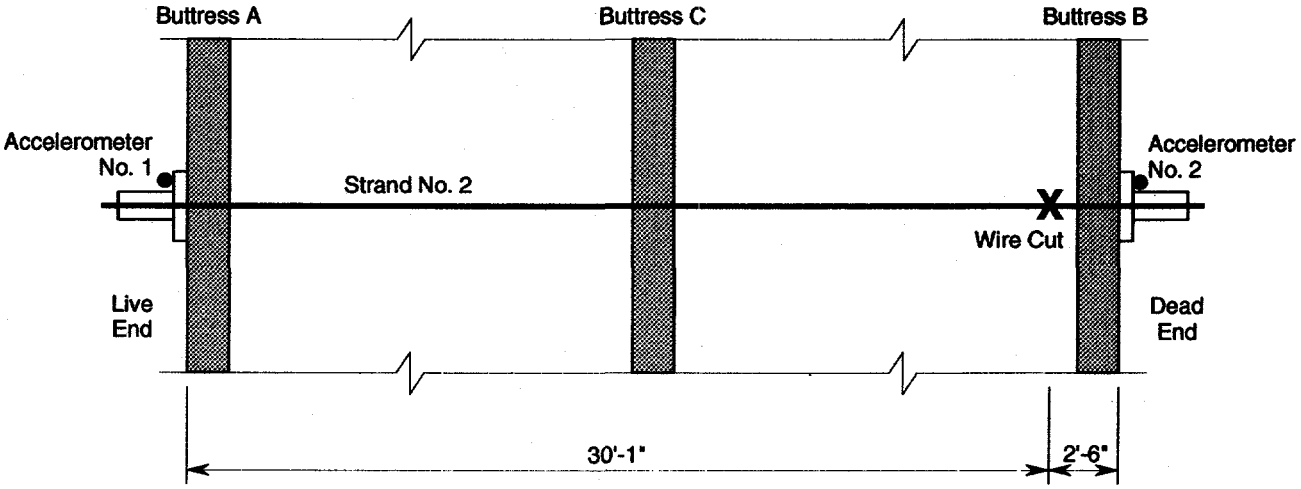

Accelerometer and Wire Cut Locations for Test No.'s 5, 6, 7, 8 and 9

Figure 9. Details of test (Tests 1 through 9).

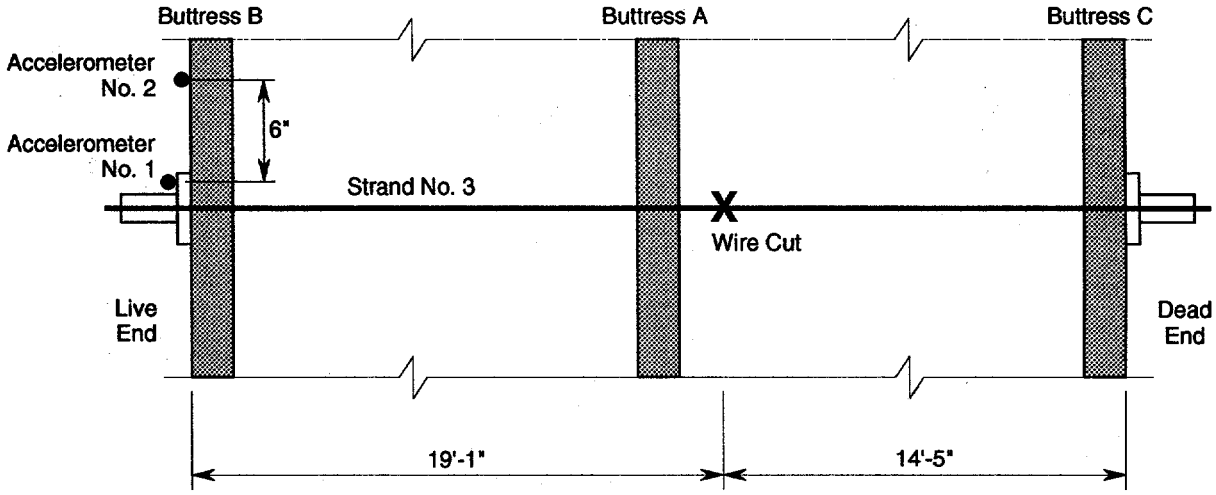

Accelerometer and Wire Cut Locations for Test No.'s 10, 11, 12, 13 and 14

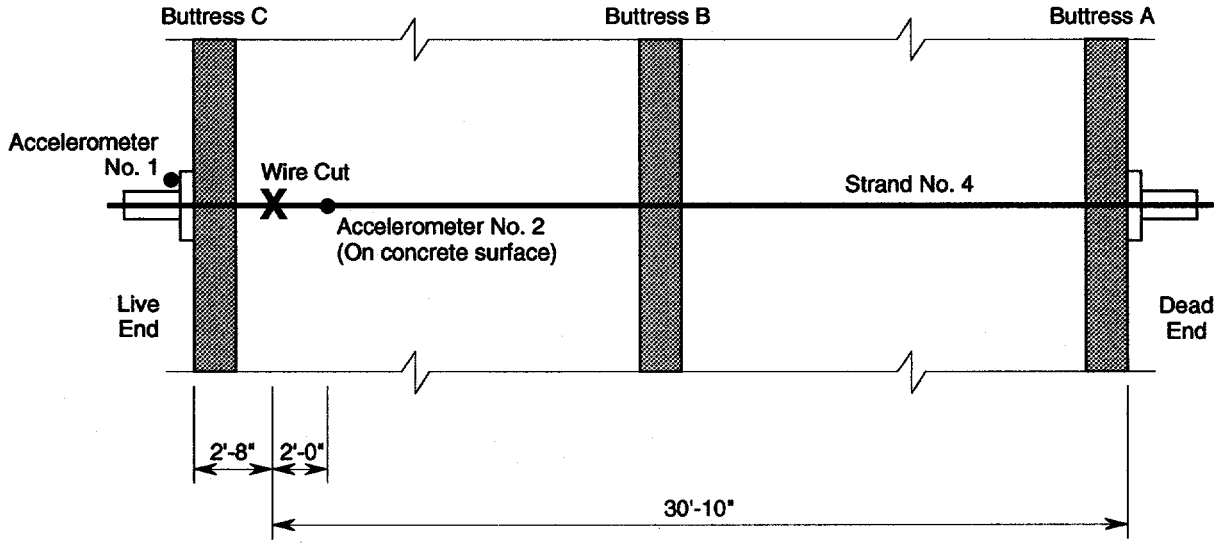

Accelerometer and Wire Cut Locations for Test No.'s 15, 16, 17 and 18

Figure 10. Details of test (Tests 10 through 18).

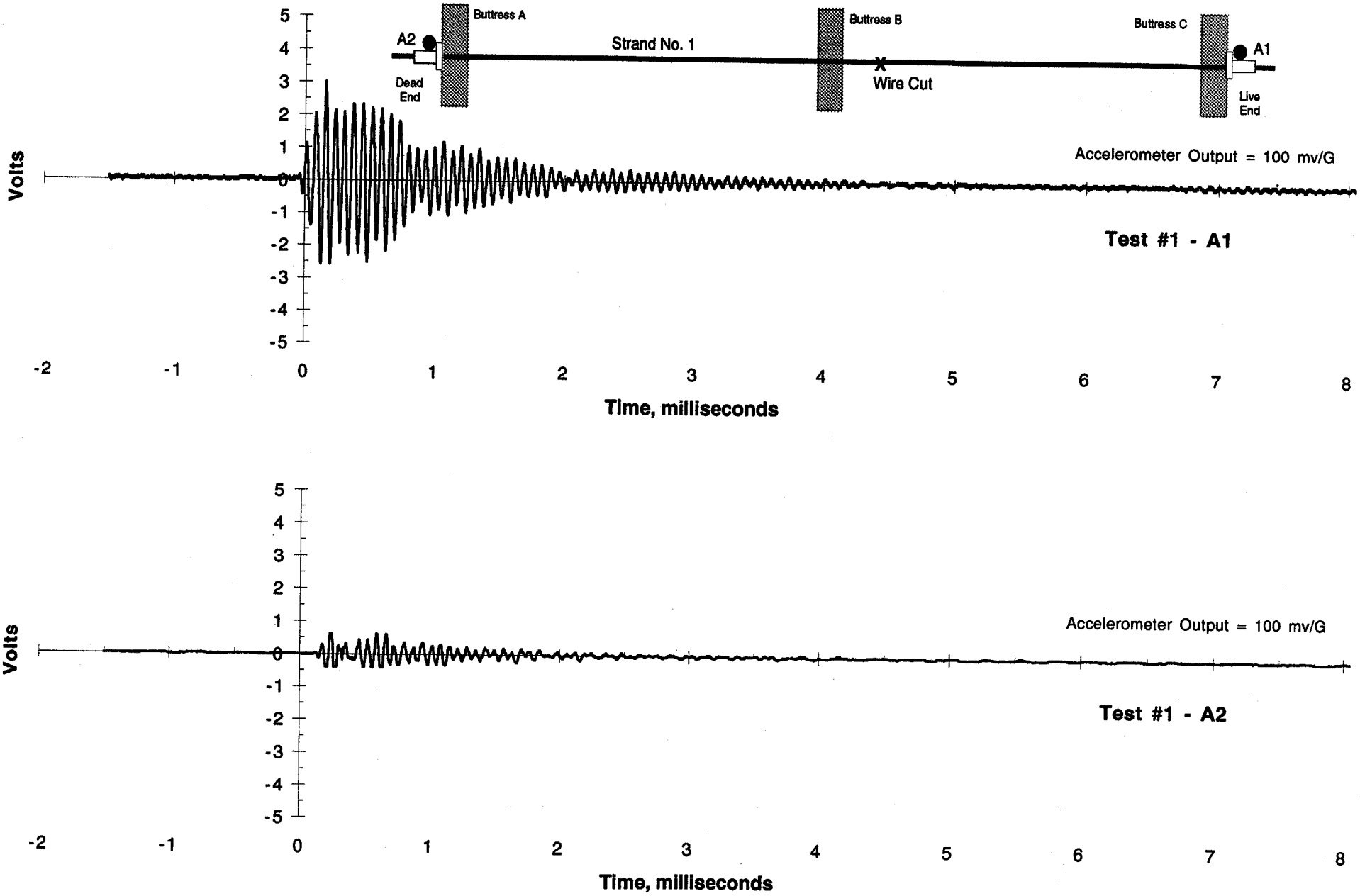

Figure 11. Time domain response of A1 and A2 in Test No. 1.

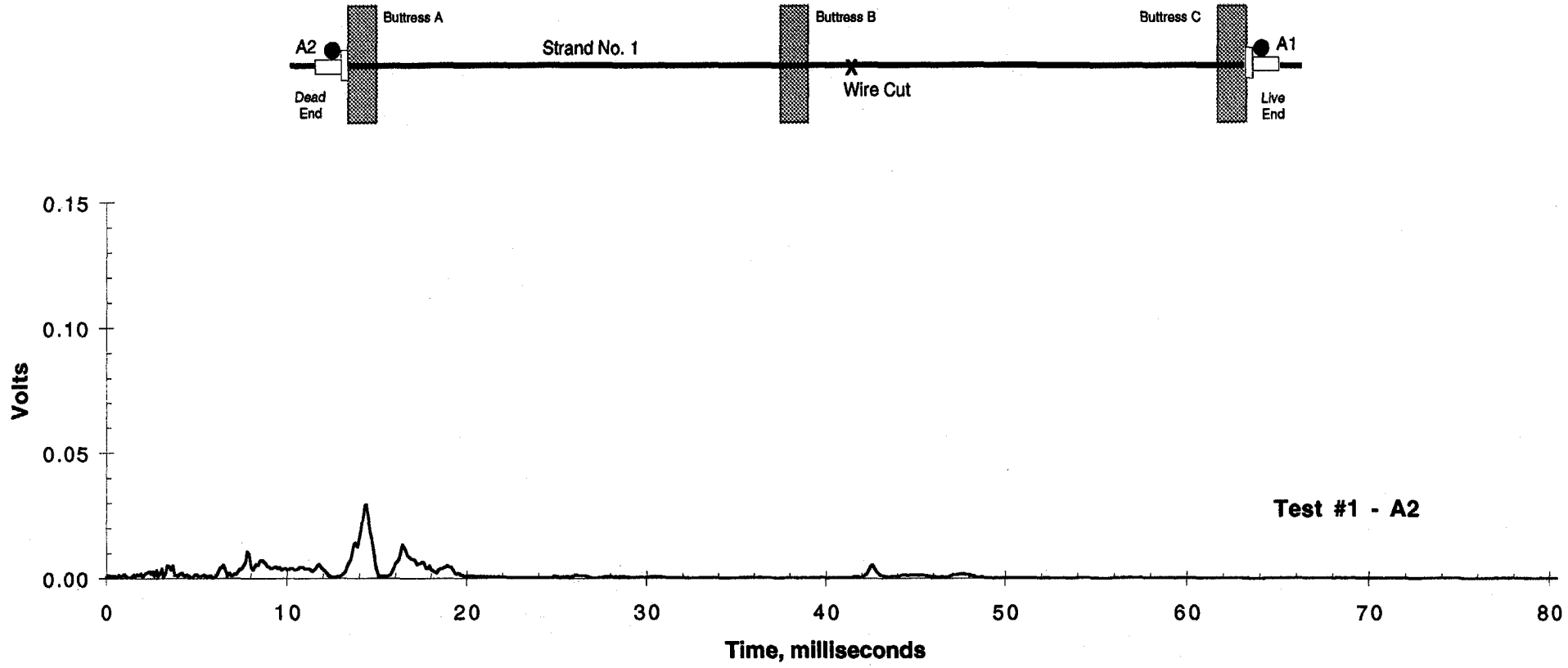

Figure 12. Frequency domain response of A2 in Test No. 1.

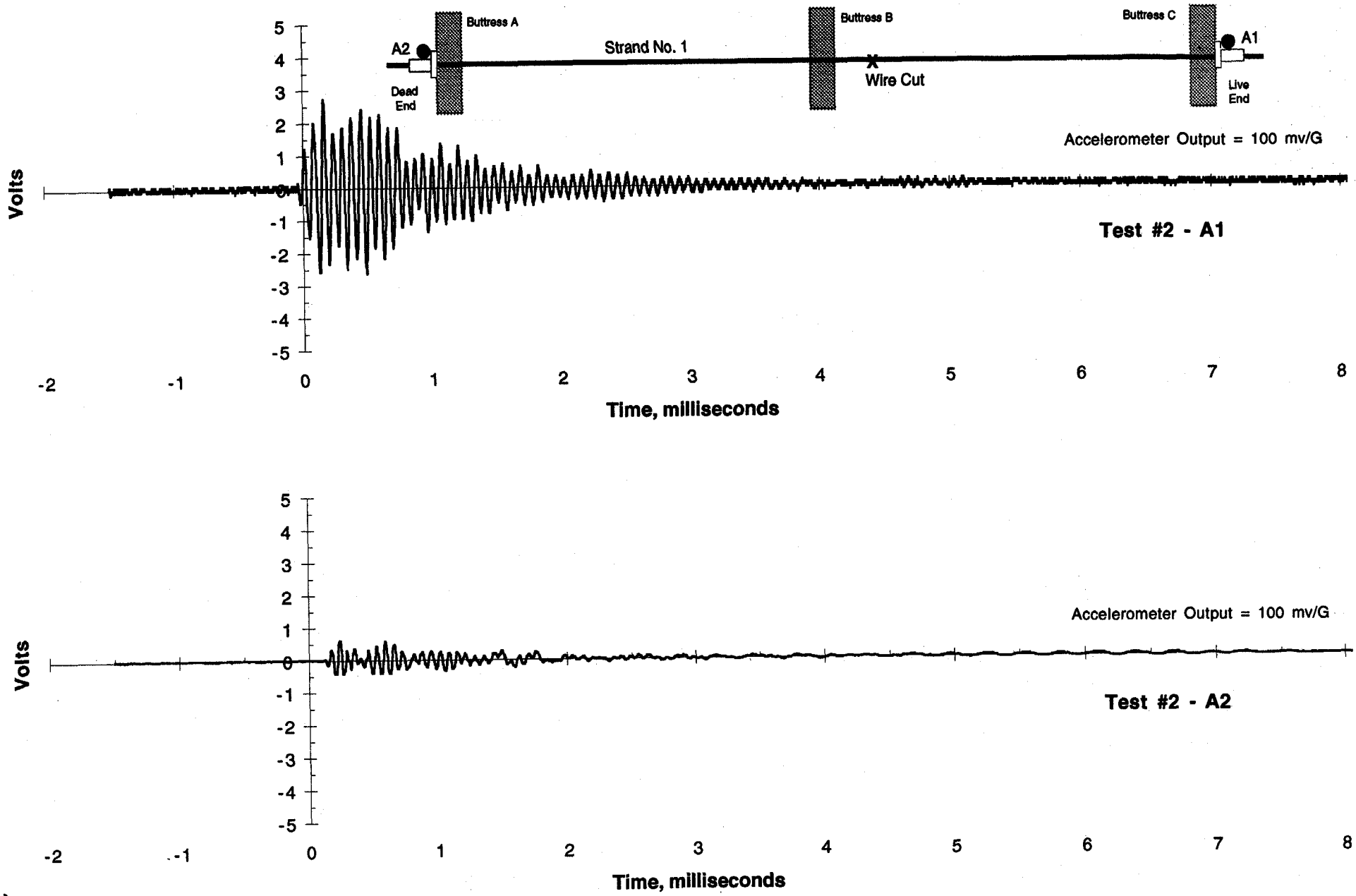

Figure 13. Time domain response of A1 and A2 in Test No. 2.

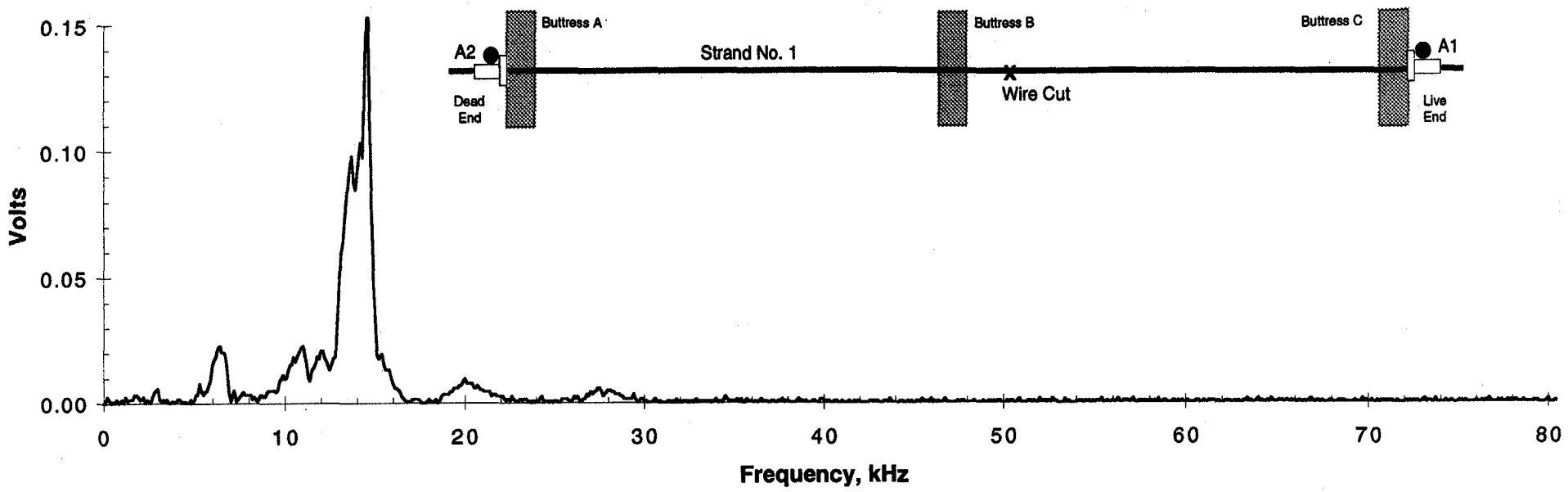

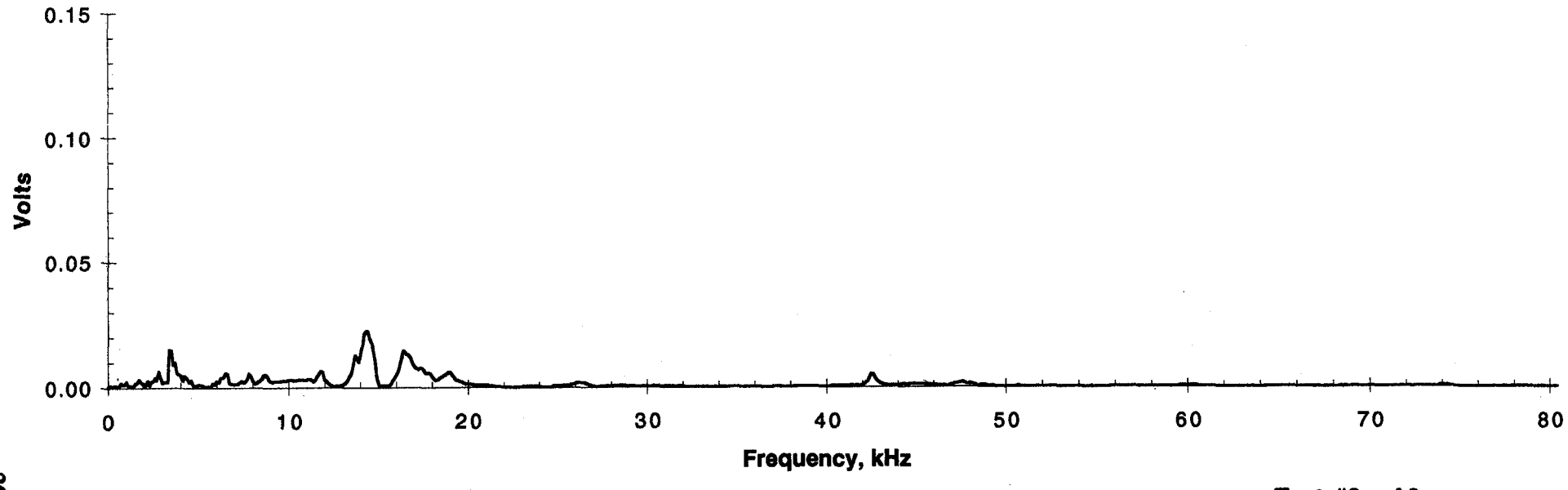

Figure 14. Frequency domain response of A1 and A2 in Test No. 2.

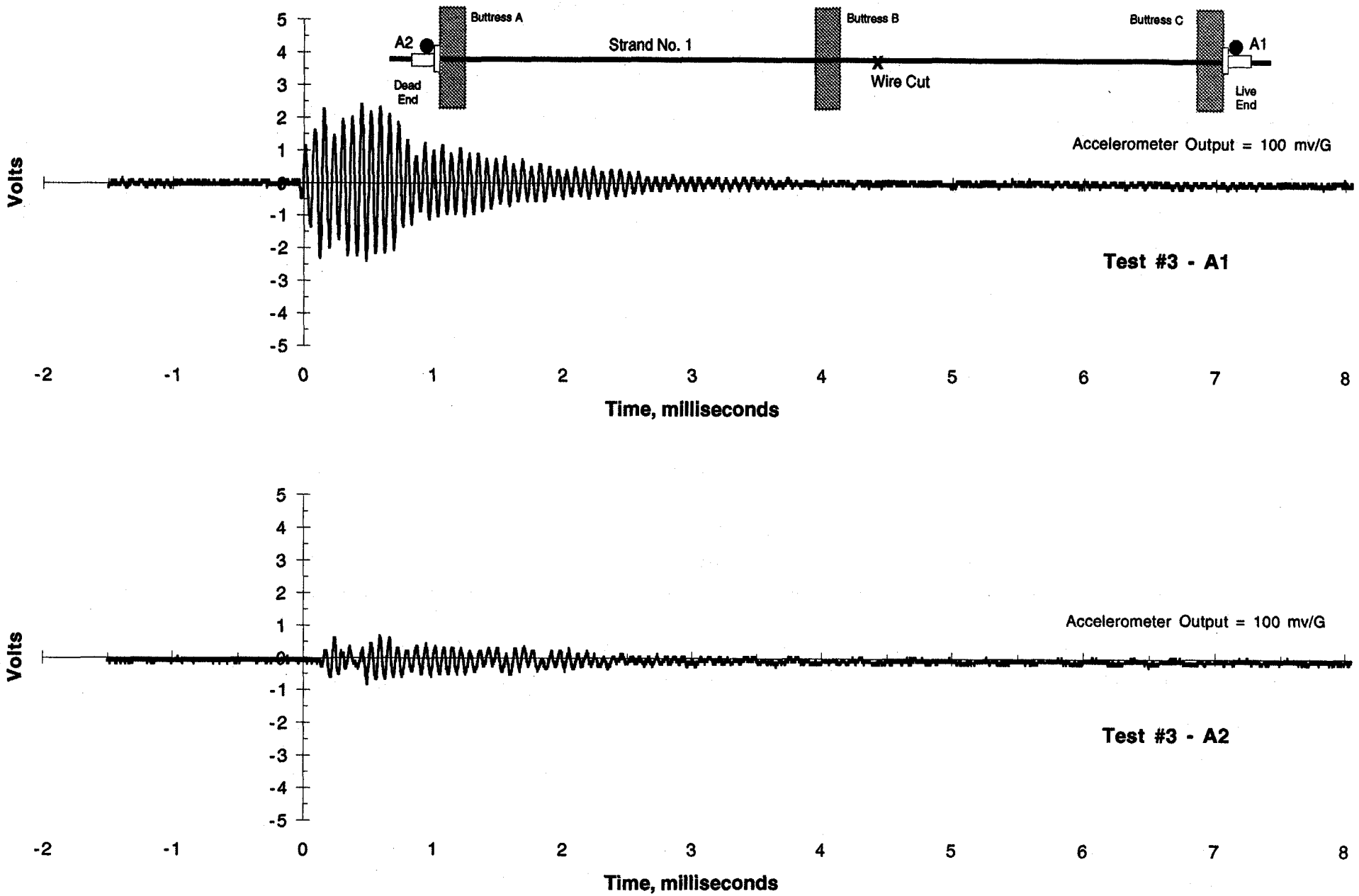

Figure 15. Time domain response of A1 and A2 in Test No. 3.

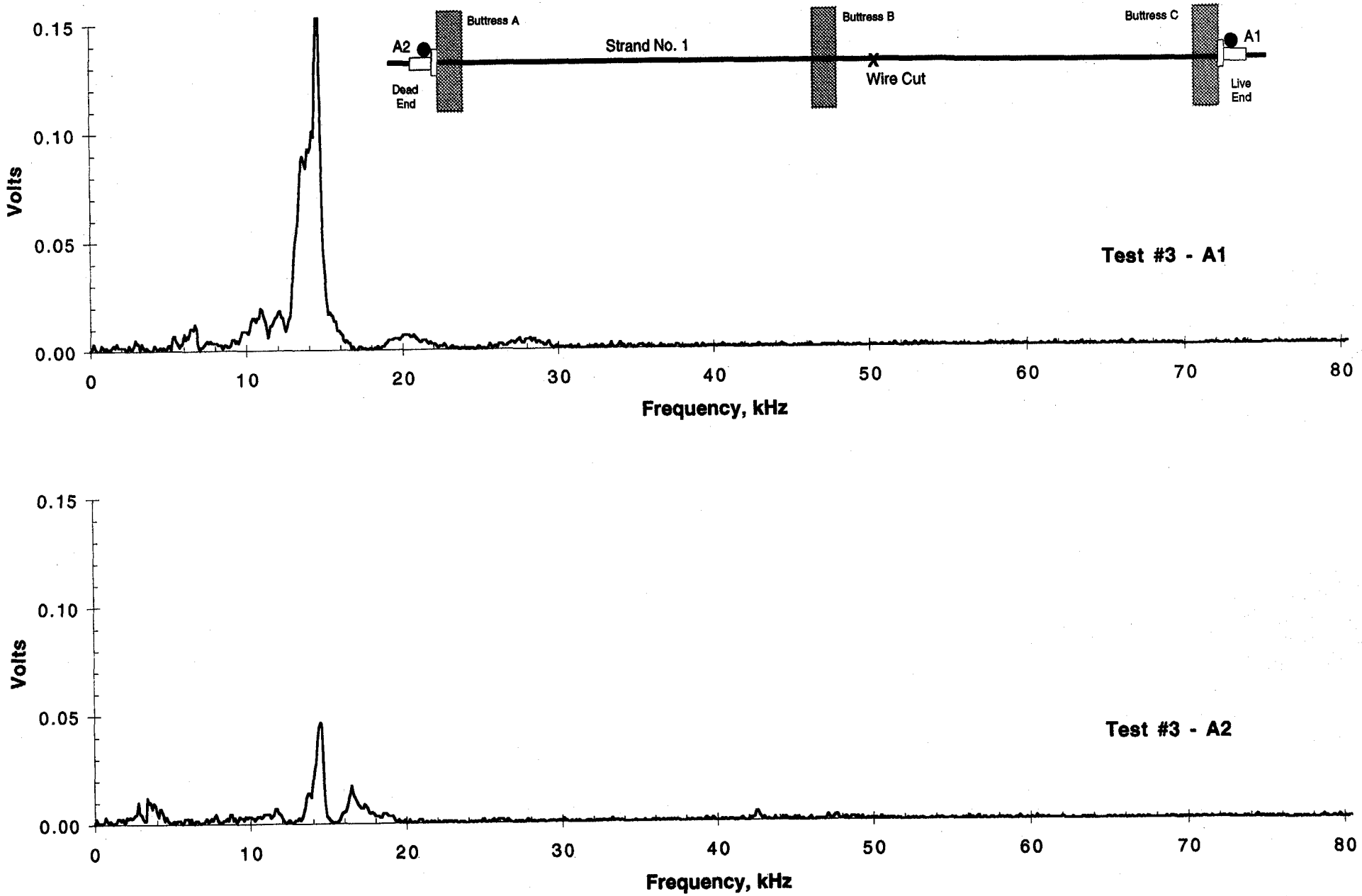

Figure 16. Frequency domain response of A1 and A2 in Test No. 3.

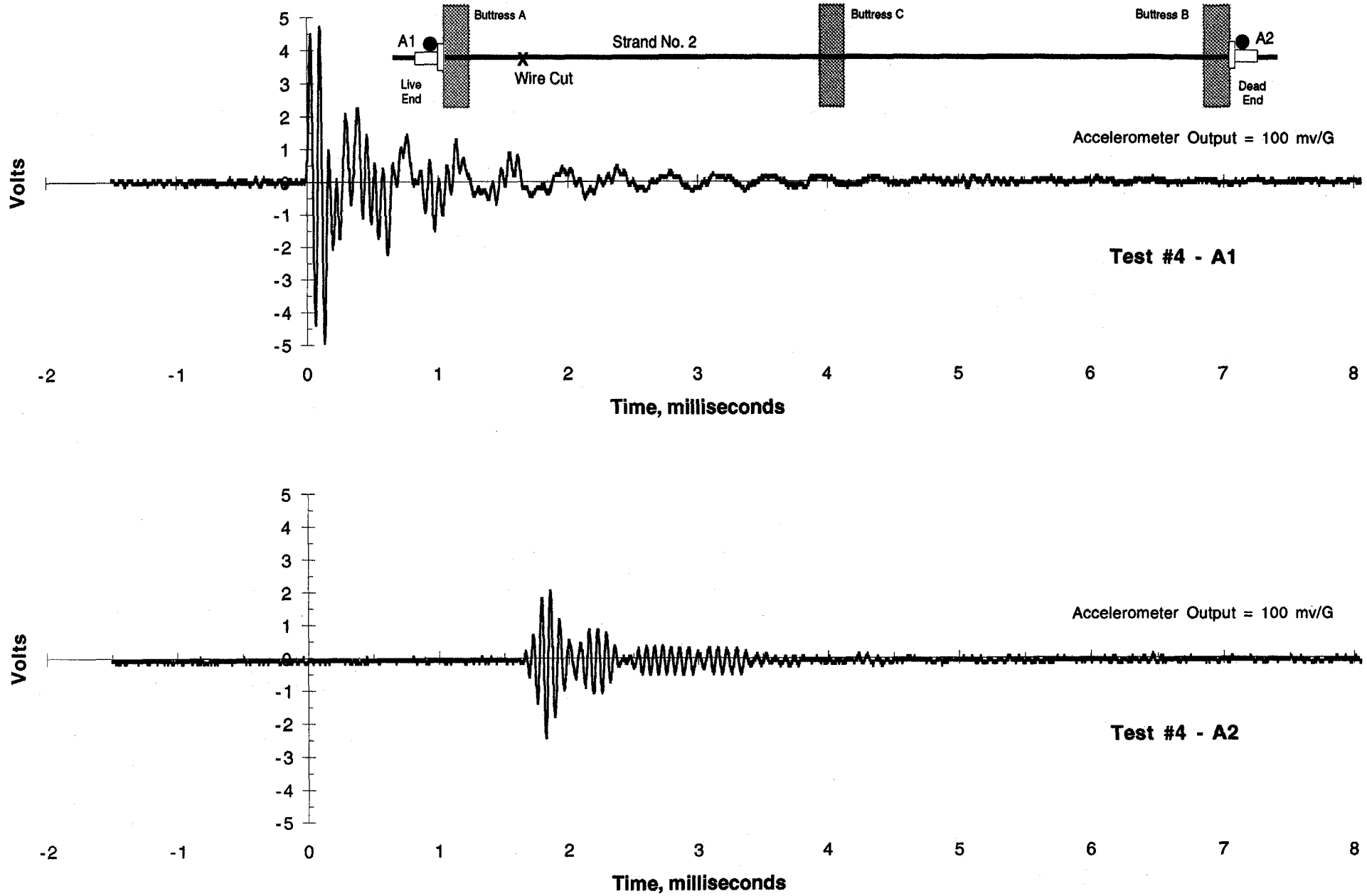

Figure 17. Time domain response of A1 and A2 in Test No. 4.

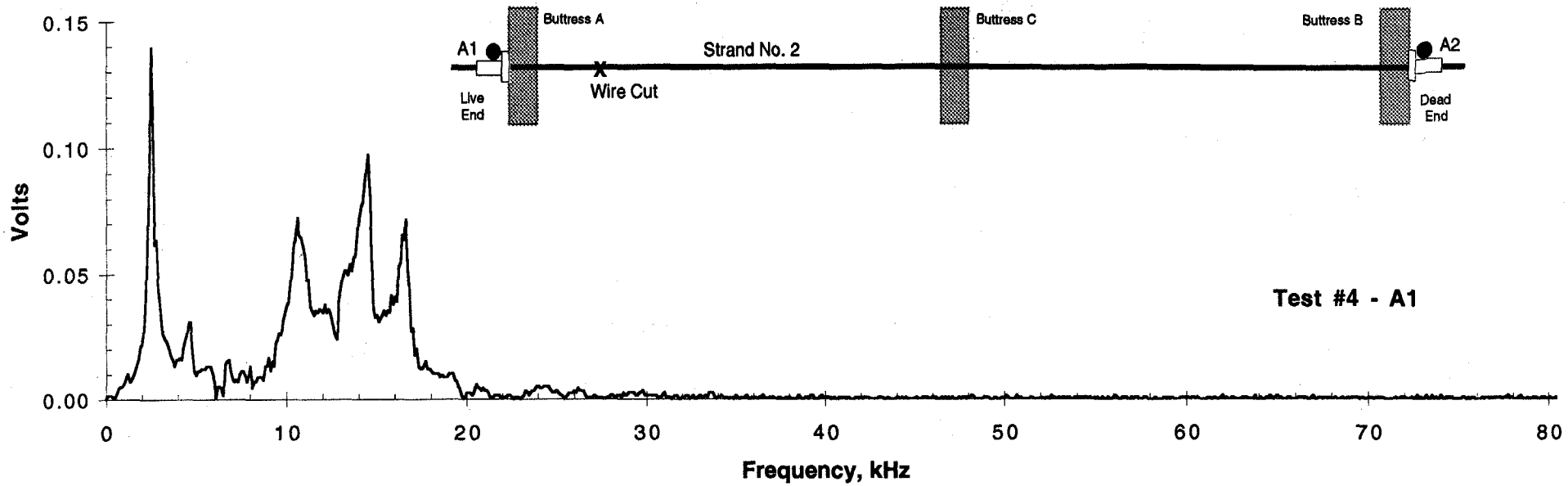

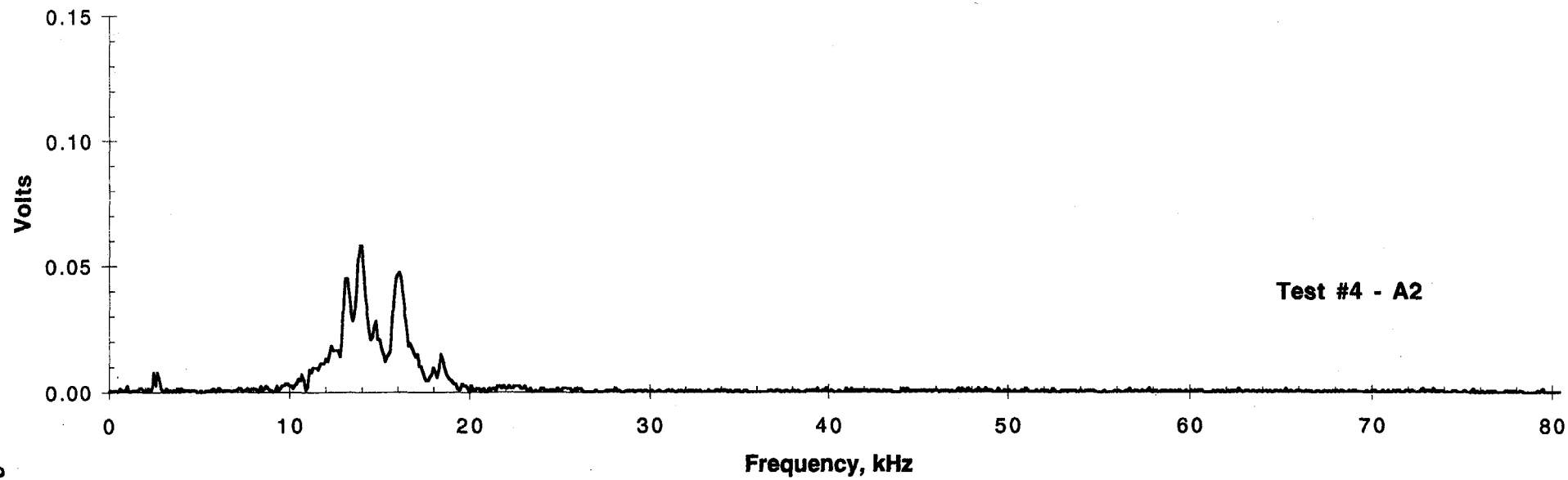

Figure 18. Frequency domain response of A1 and A2 in Test No. 4.

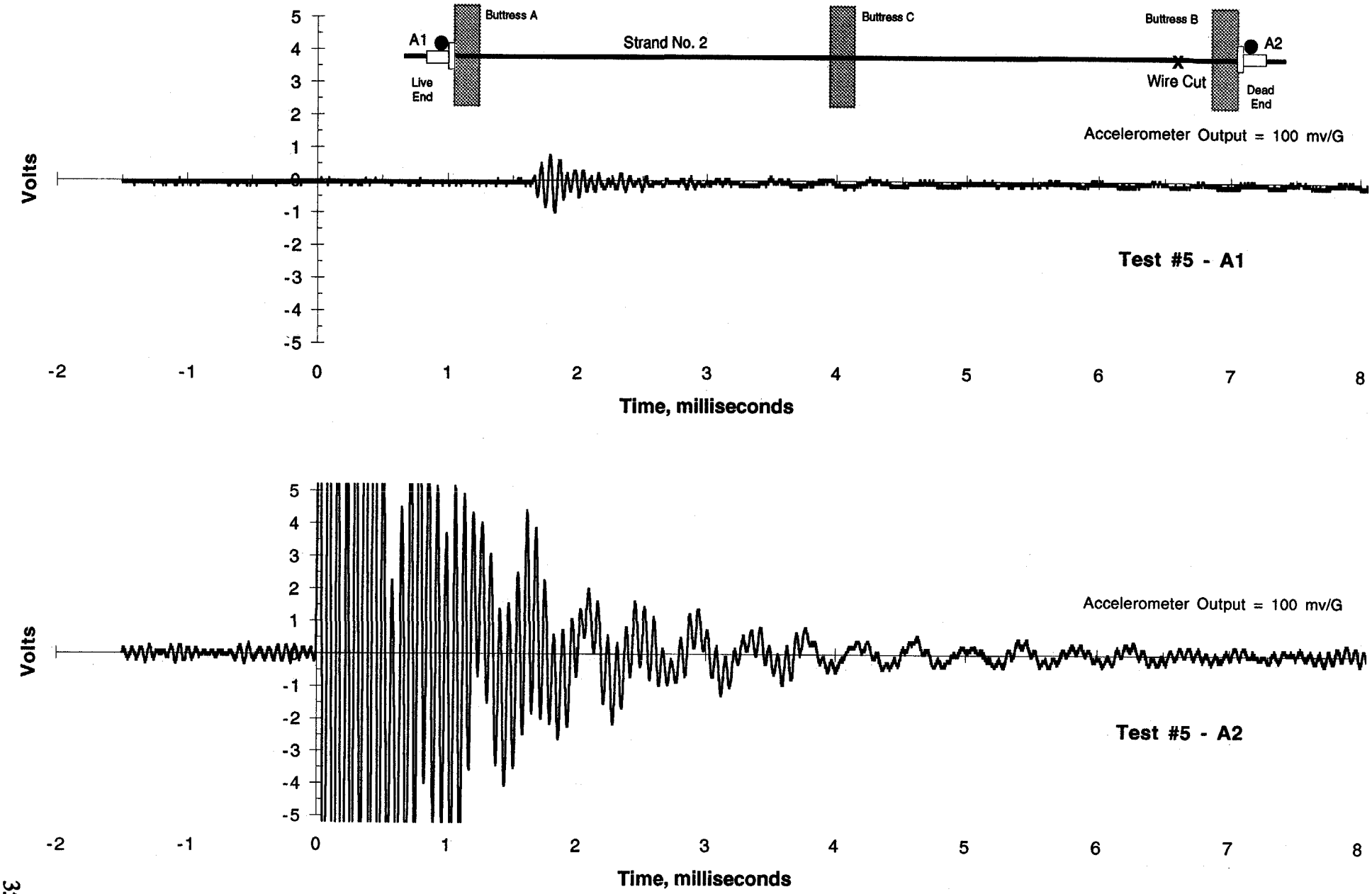

Figure 19. Time domain response of A1 and A2 in Test No. 5.

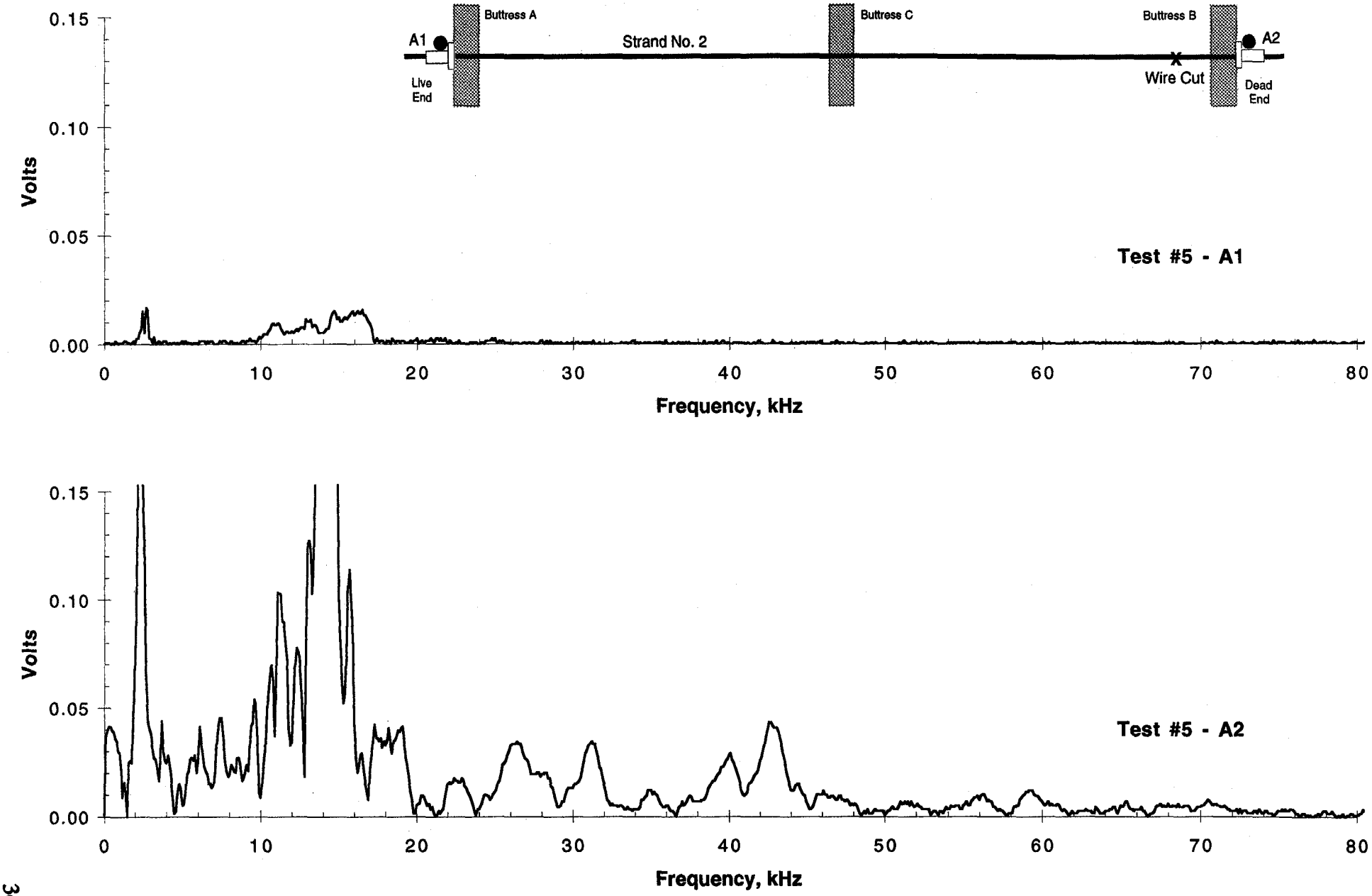

Figure 20. Frequency domain response of A1 and A2 in Test No. 5.

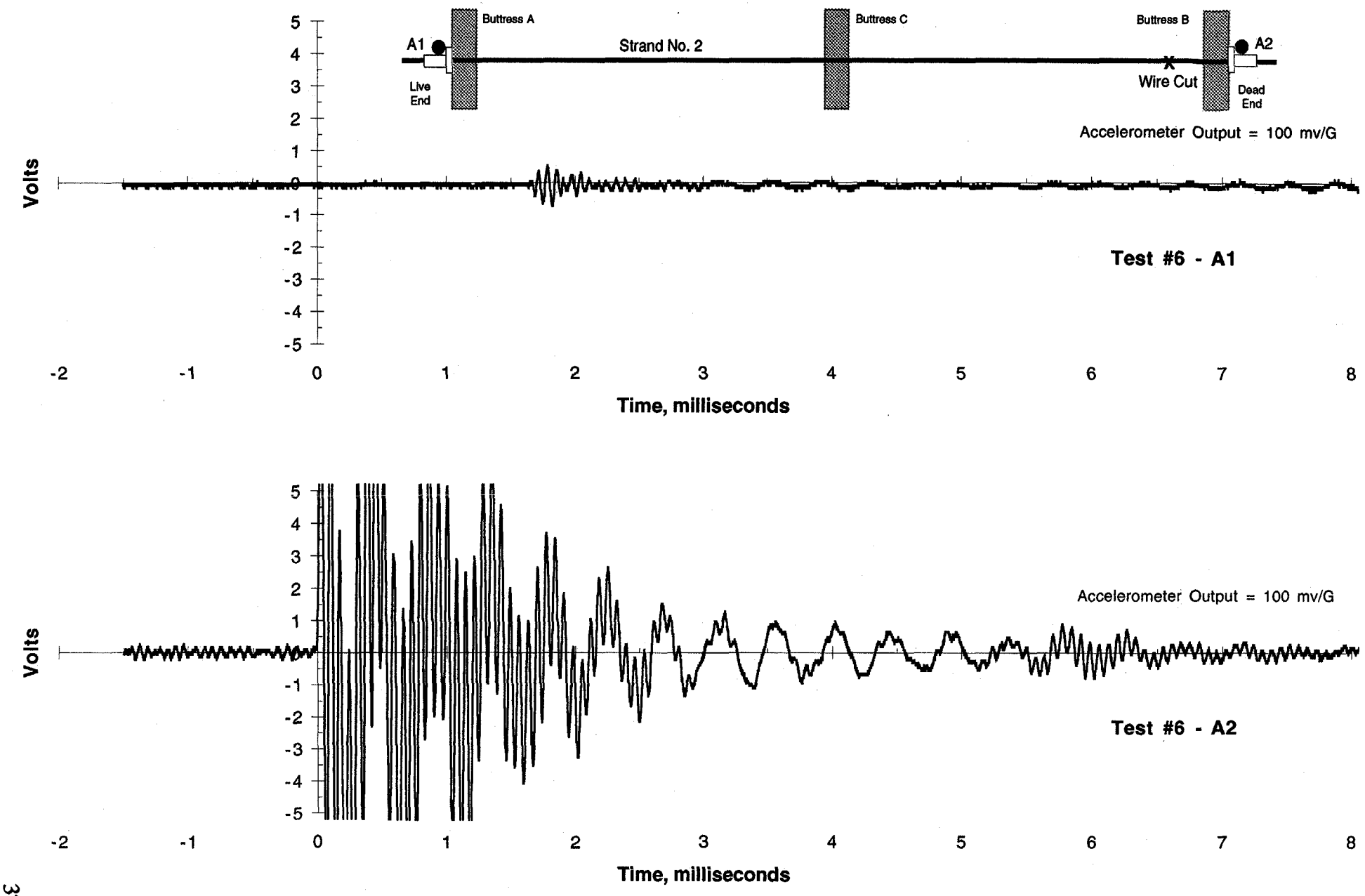

Figure 21. Time domain response of A1 and A2 in Test No. 6.

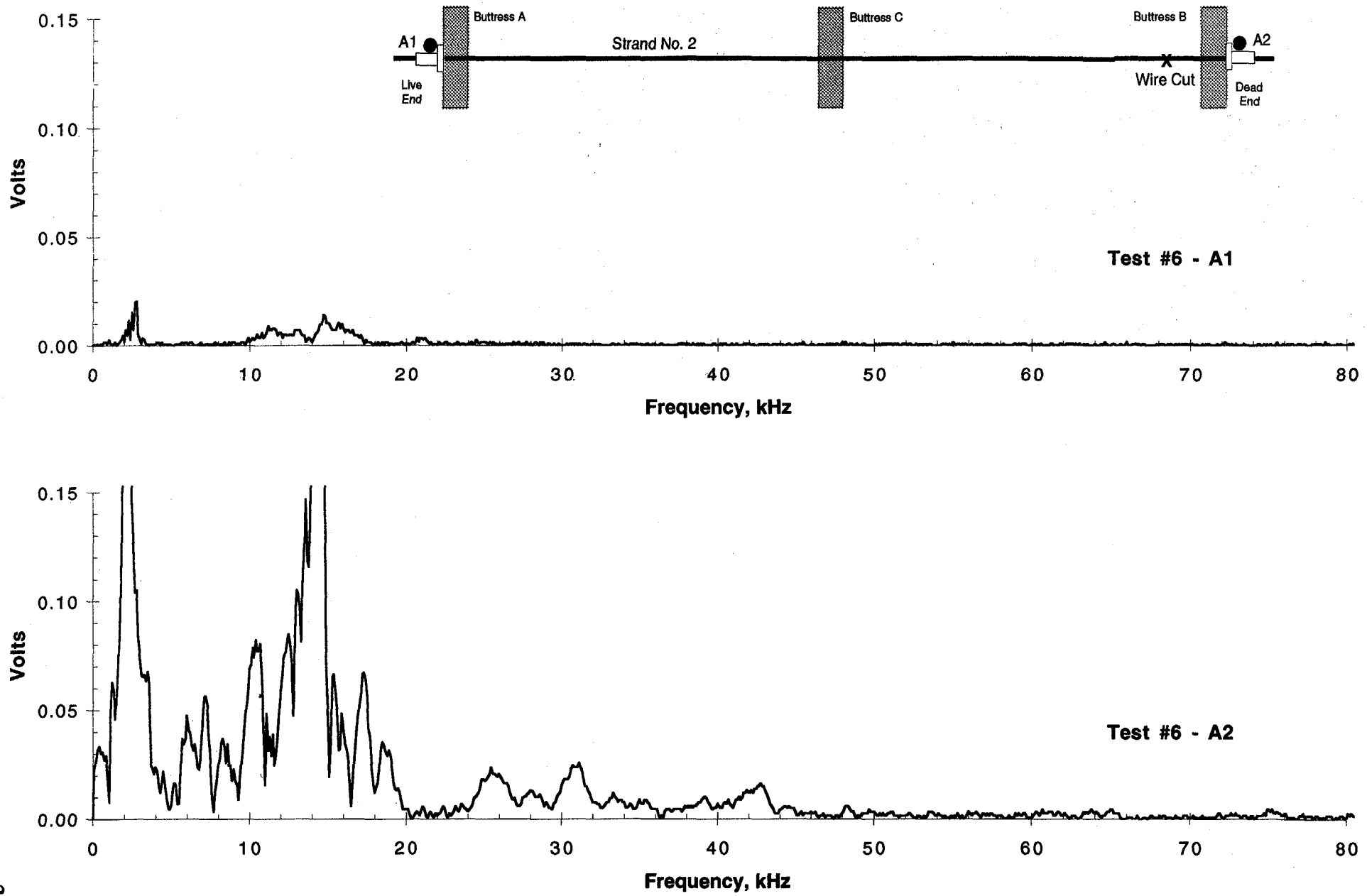

Figure 22. Frequency domain response of A1 and A2 in Test No. 6.

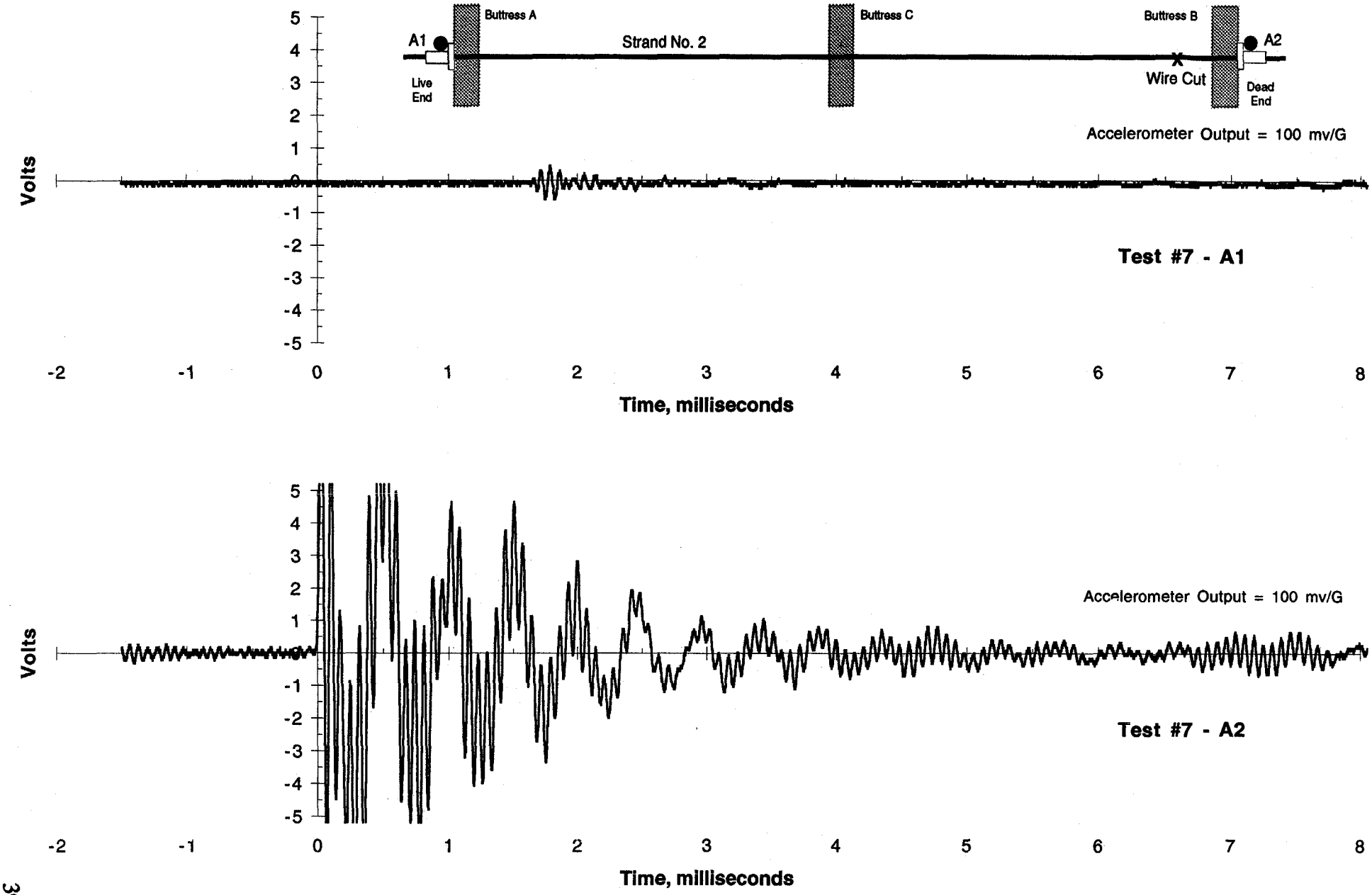

Figure 23. Time domain response of A1 and A2 in Test No. 7.

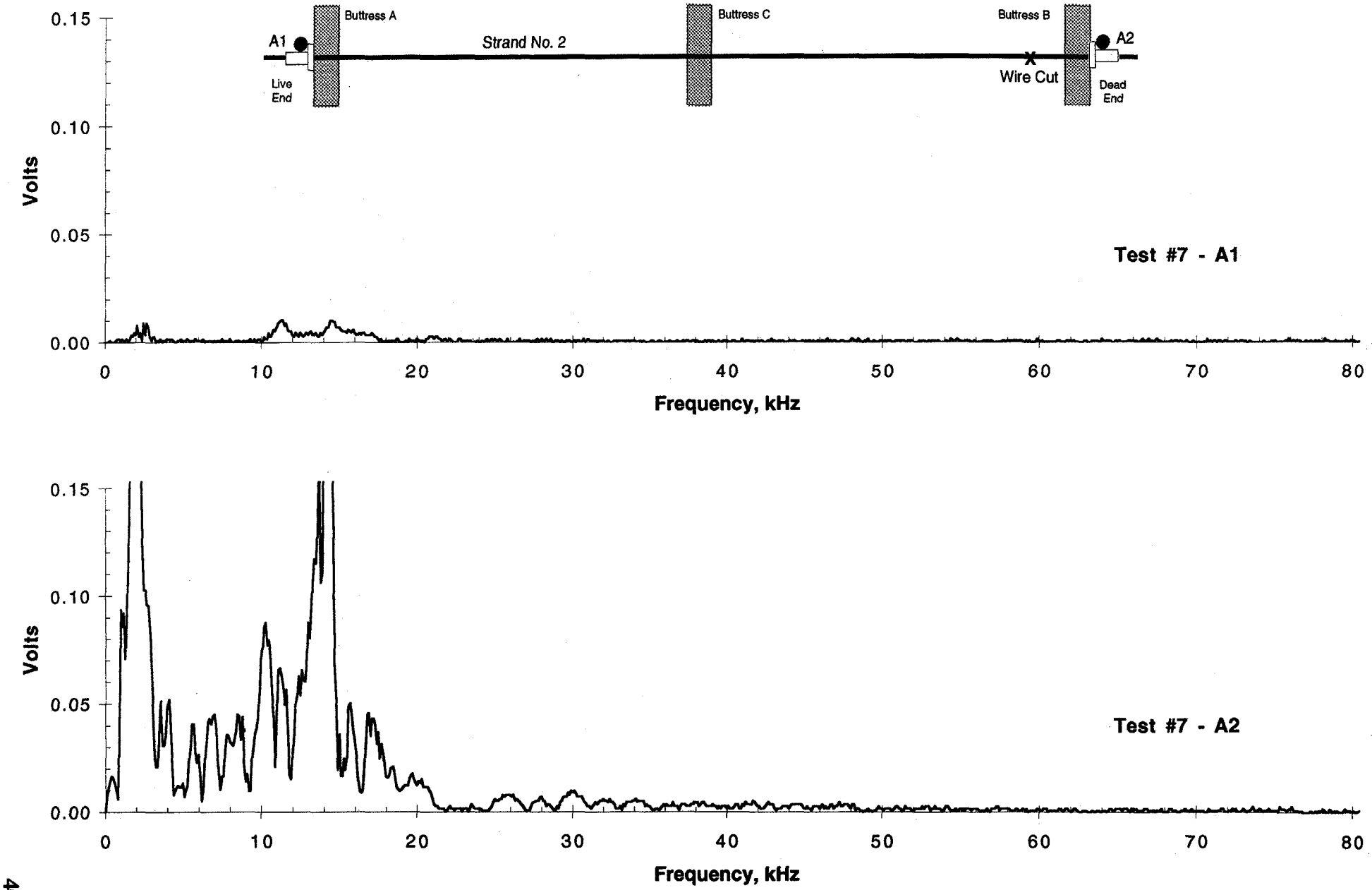

Figure 24. Frequency domain response of A1 and A2 in Test No. 7.

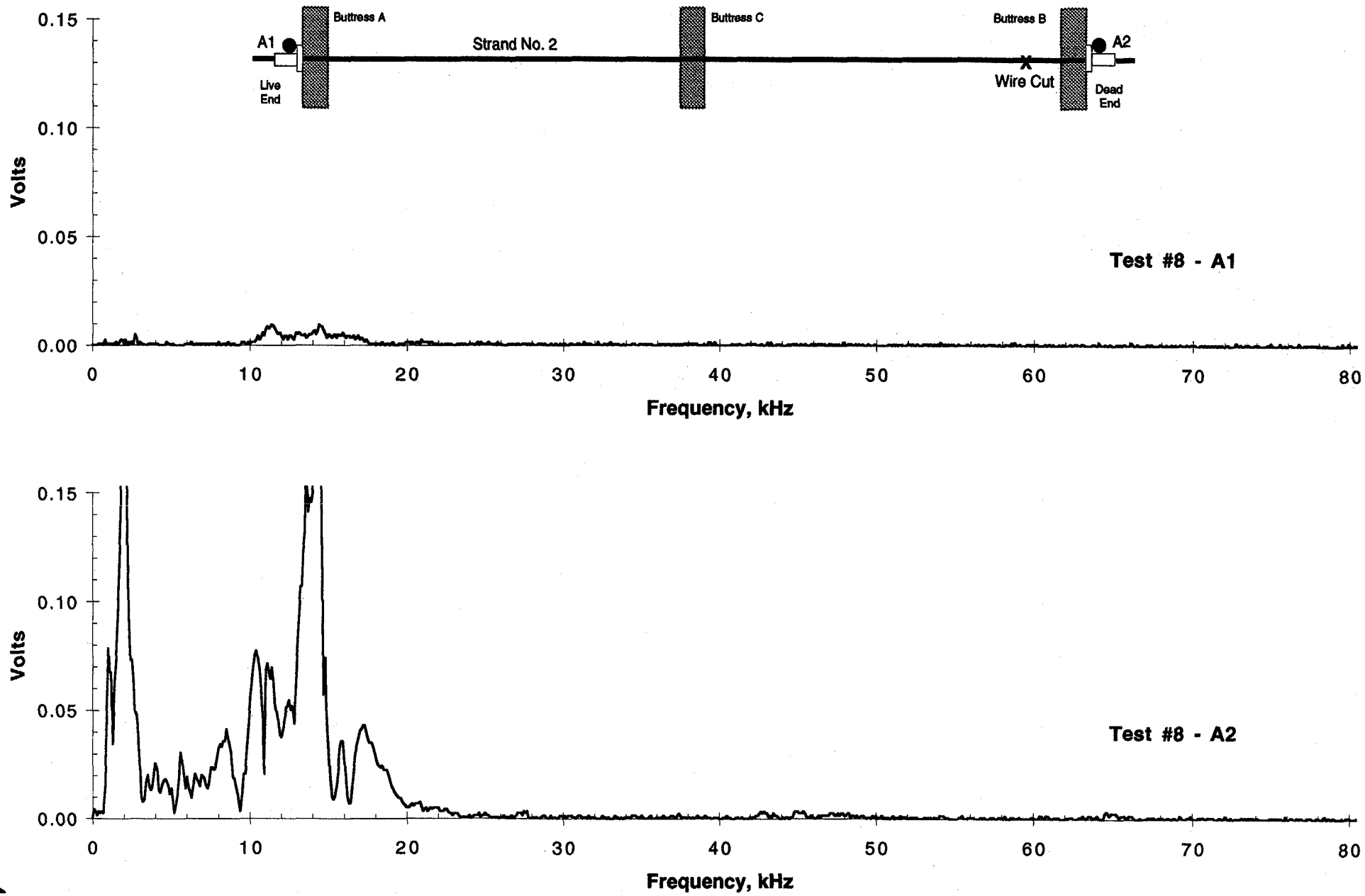

Figure 25. Time domain response of A1 and A2 in Test No. 8.

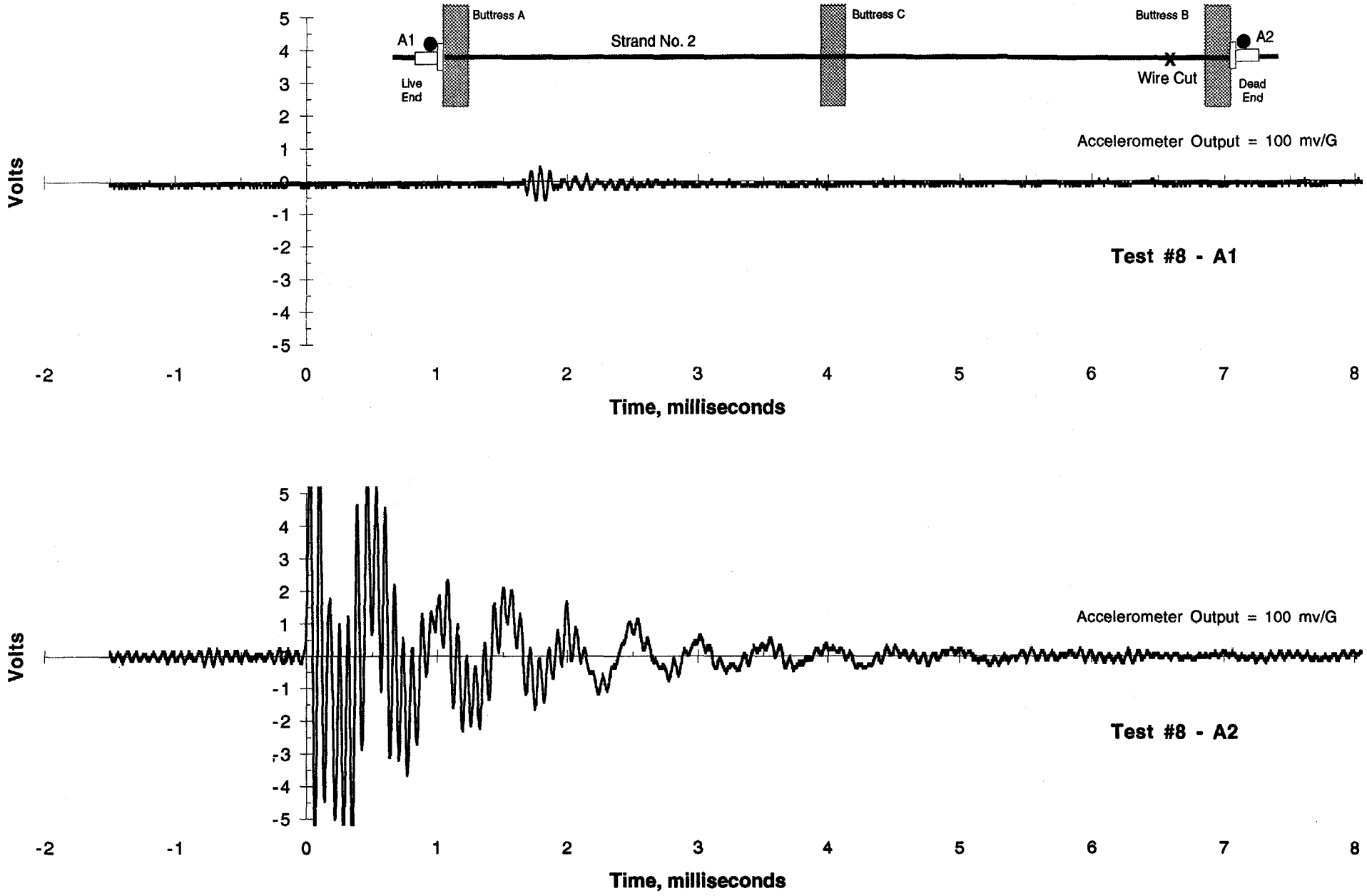

Figure 26. Frequency domain response of A1 and A2 in Test No. 8.

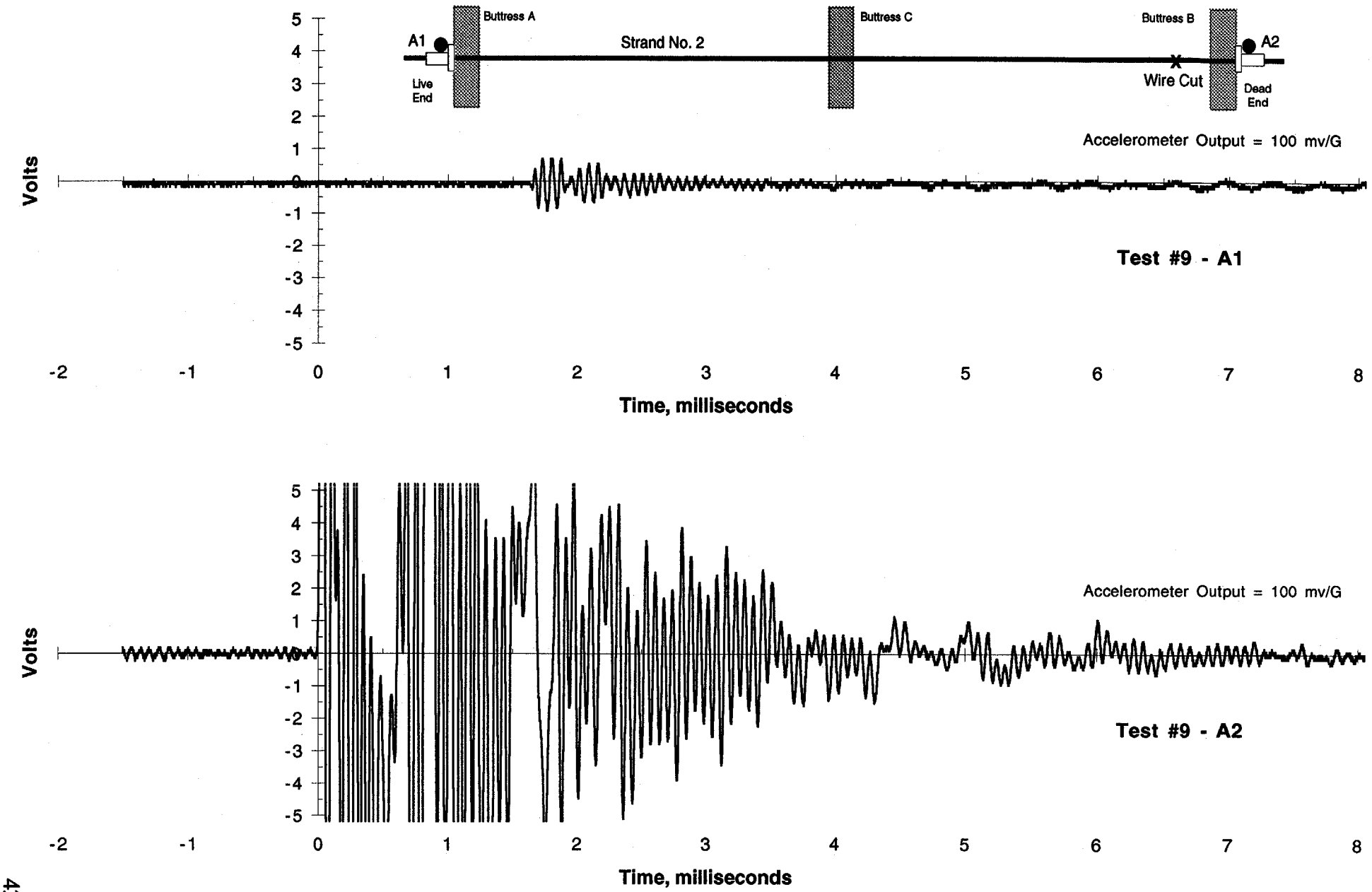

Figure 27. Time domain response of A1 and A2 in Test No. 9.

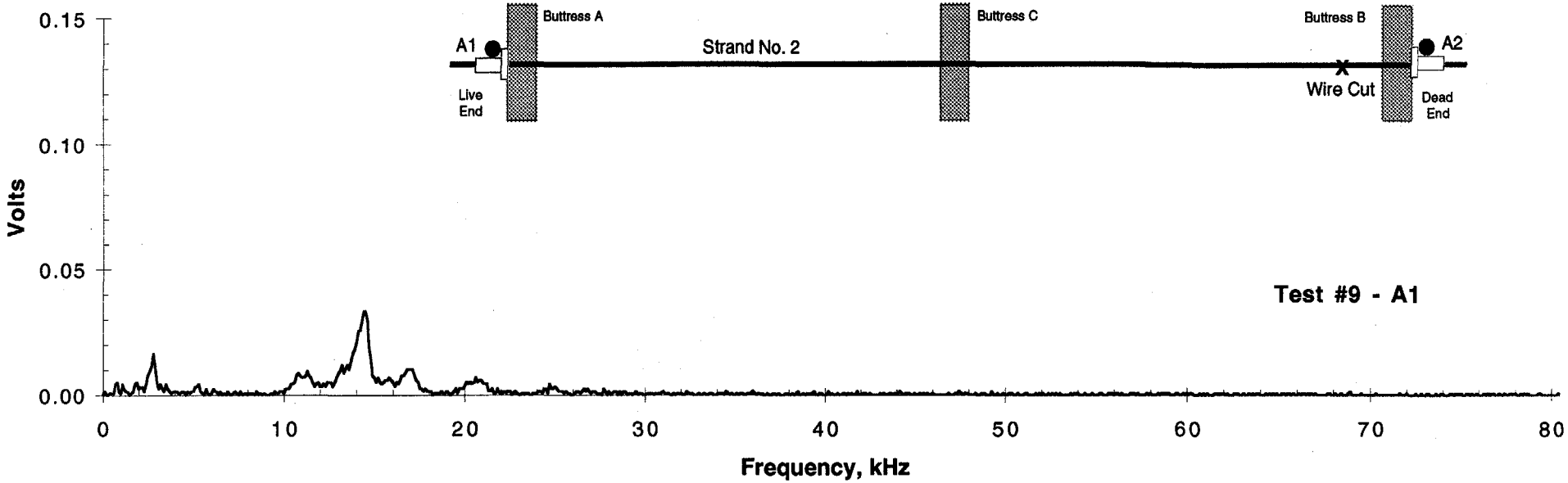

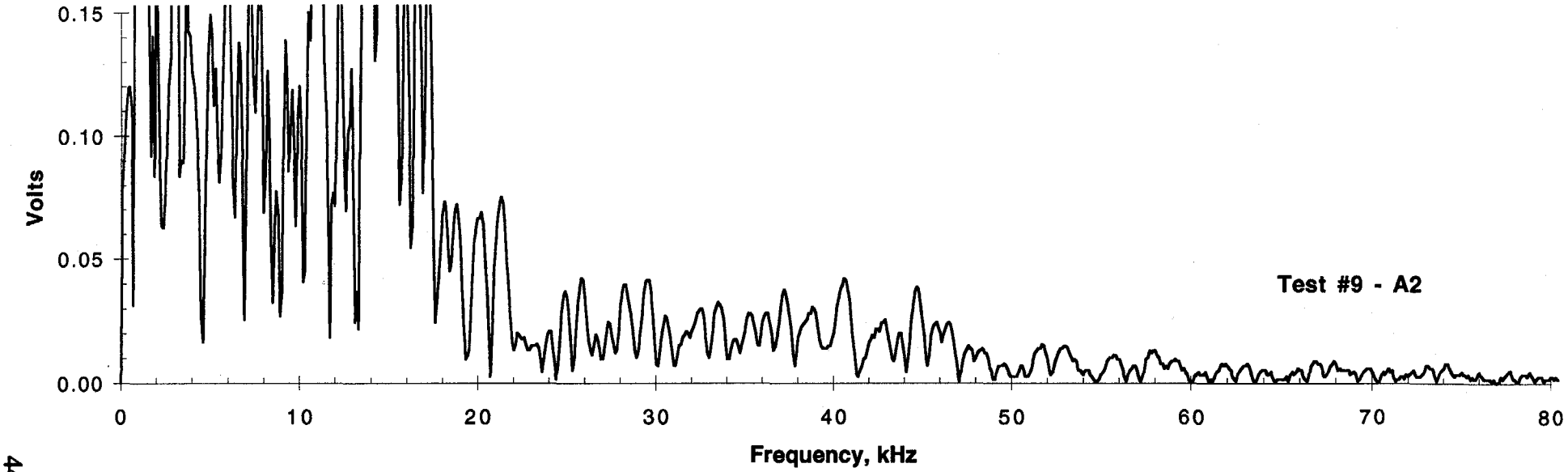

Figure 28. Frequency domain response of A1 and A2 in Test No. 9.

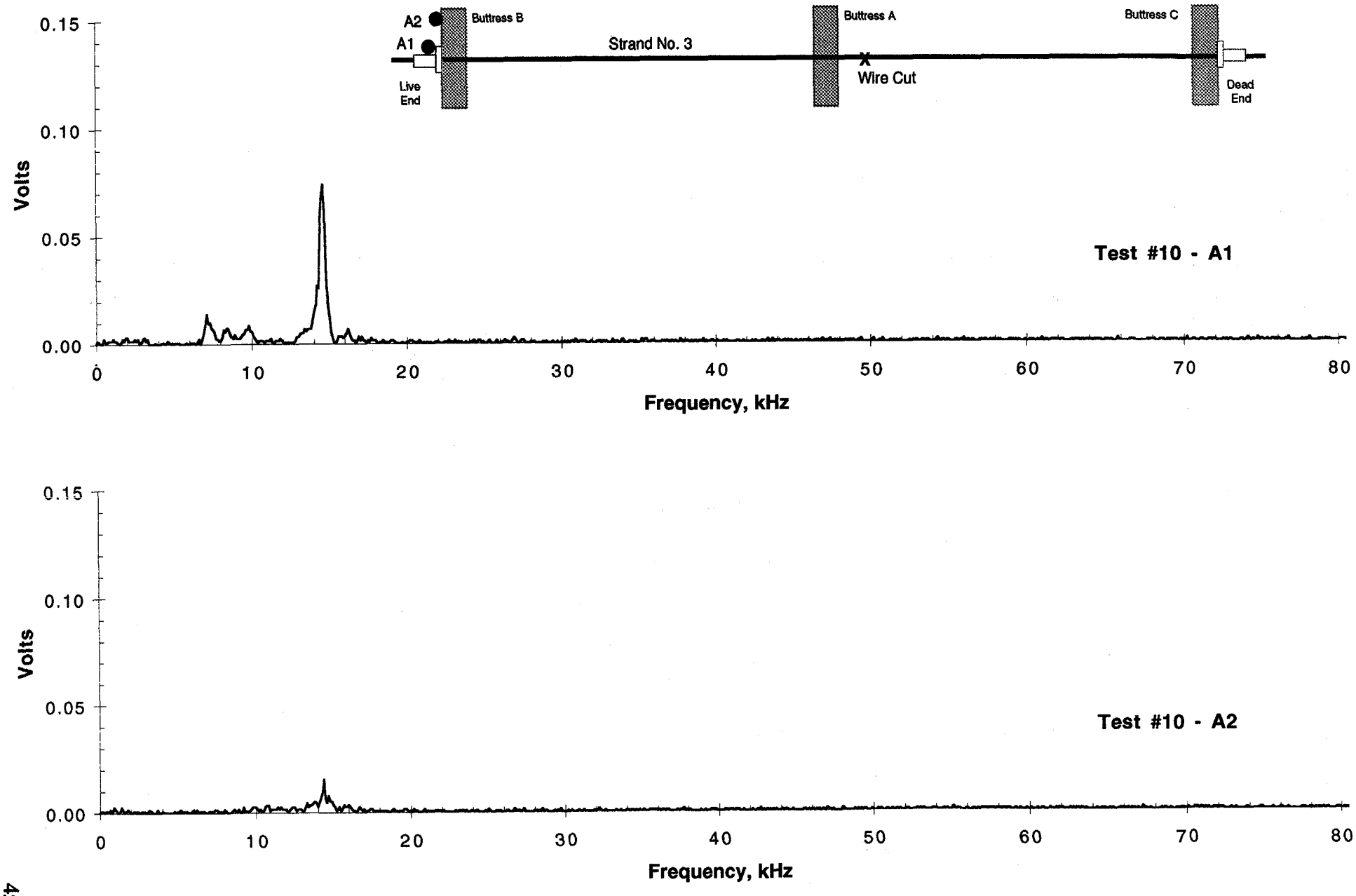

Figure 29. Time domain response of A1 and A2 in Test No. 10.

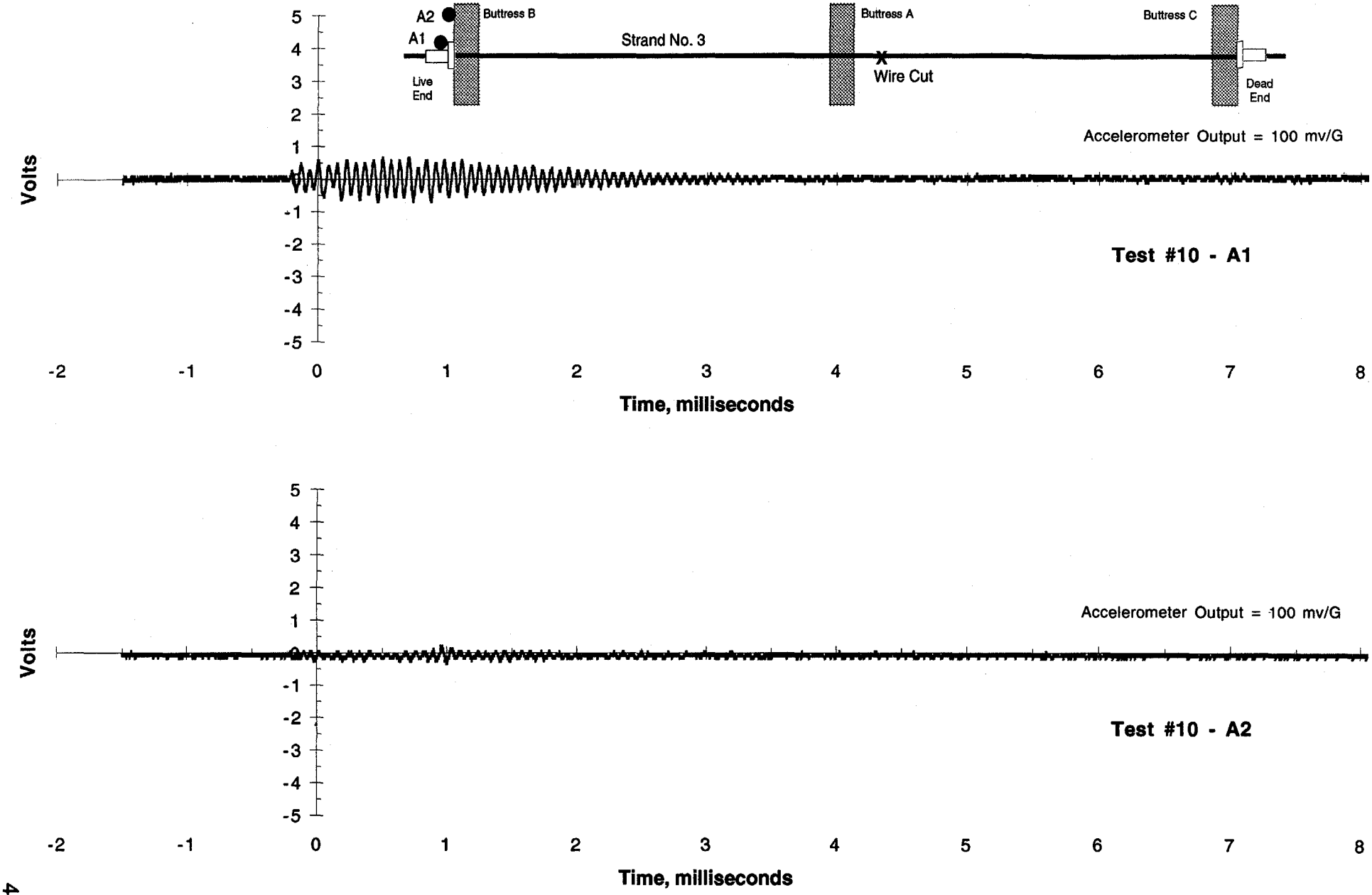

Figure 30. Frequency domain response of A1 and A2 in Test No. 10.

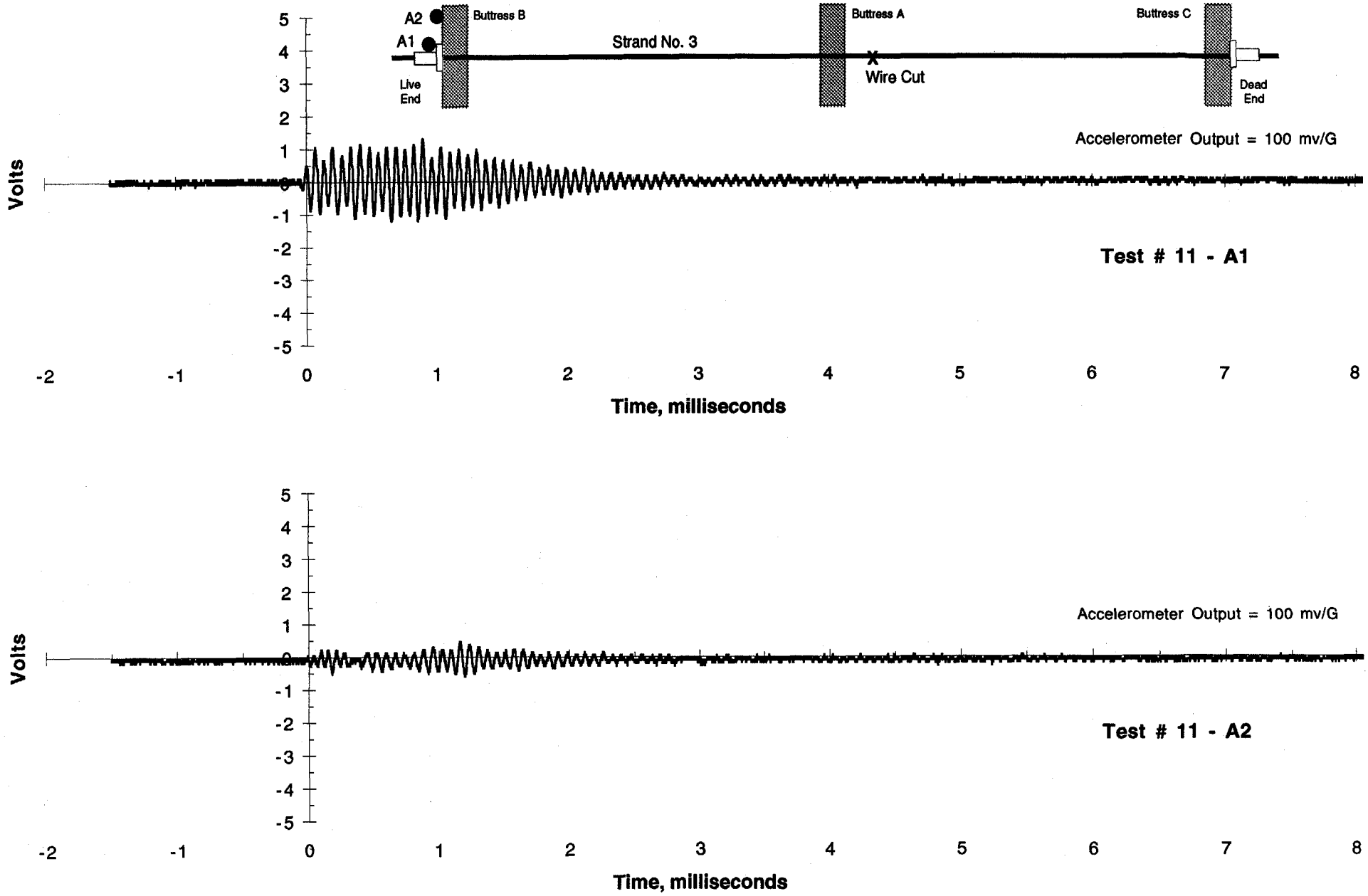

Figure 31. Time domain response of A1 and A2 in Test No. 11.

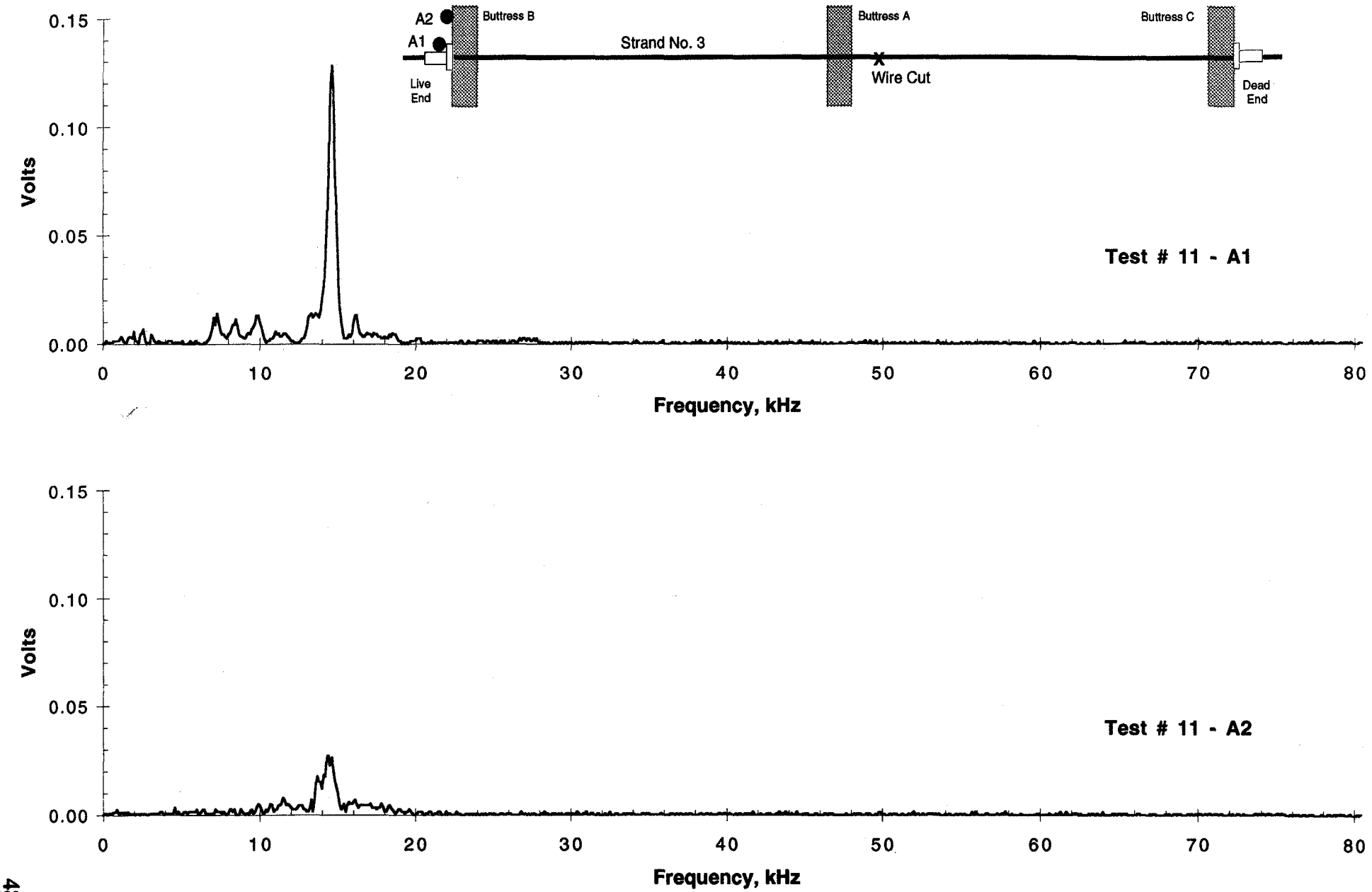

Figure 32. Frequency domain response of A1 and A2 in Test No. 11.

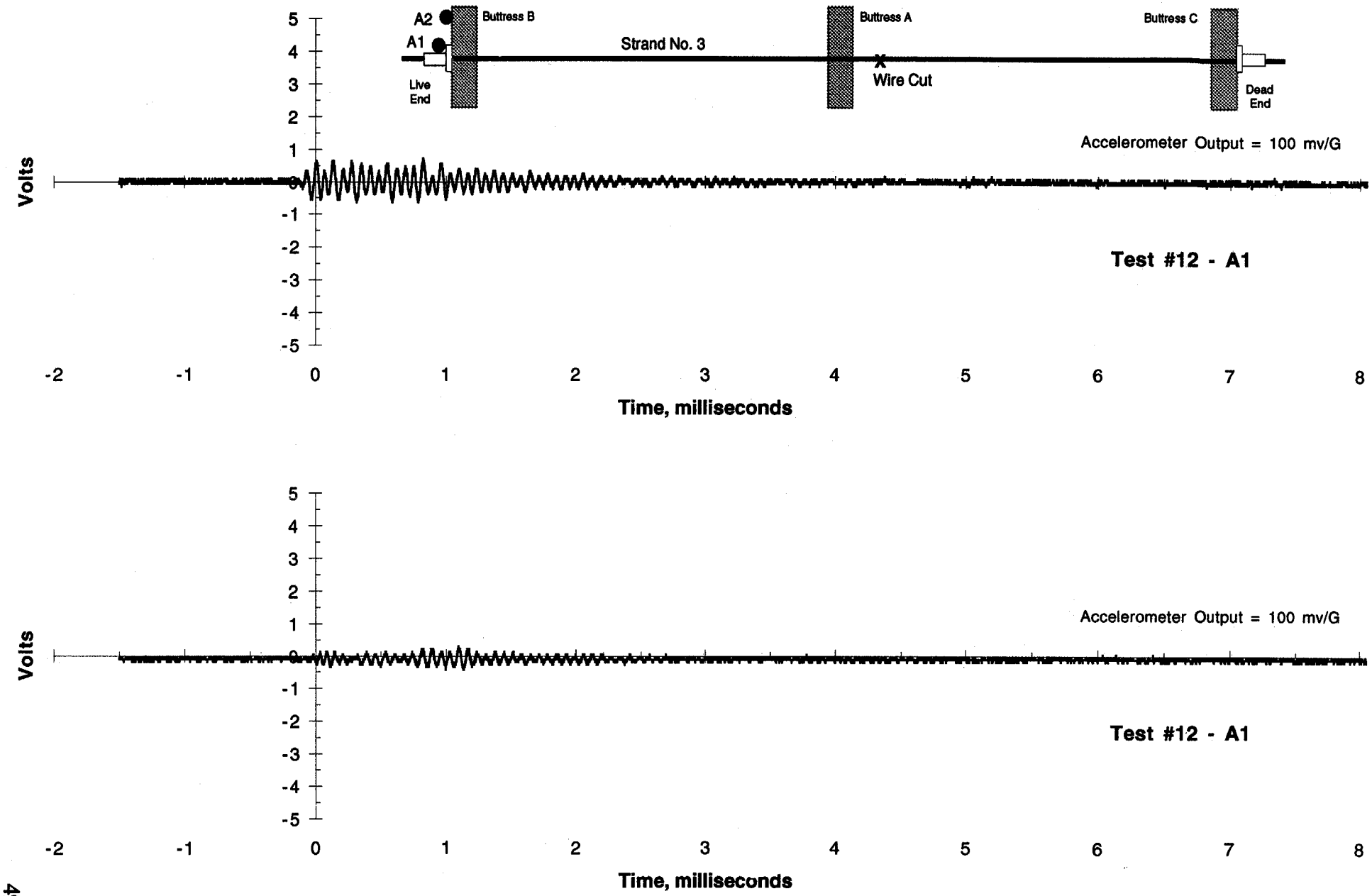

Figure 33. Time domain response of A1 and A2 in Test No. 12.

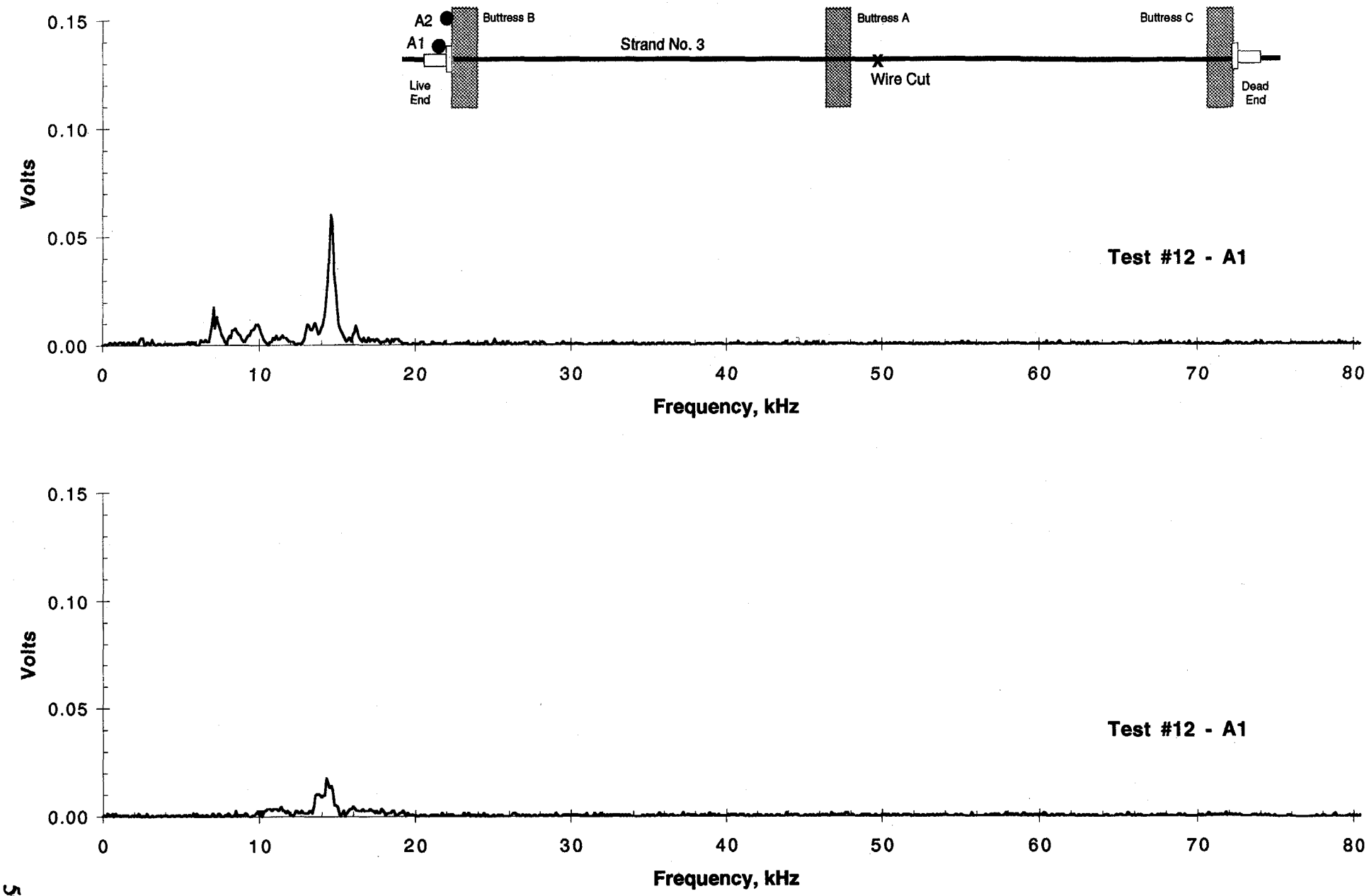

Figure 34. Frequency domain response of A1 and A2 in Test No. 12.

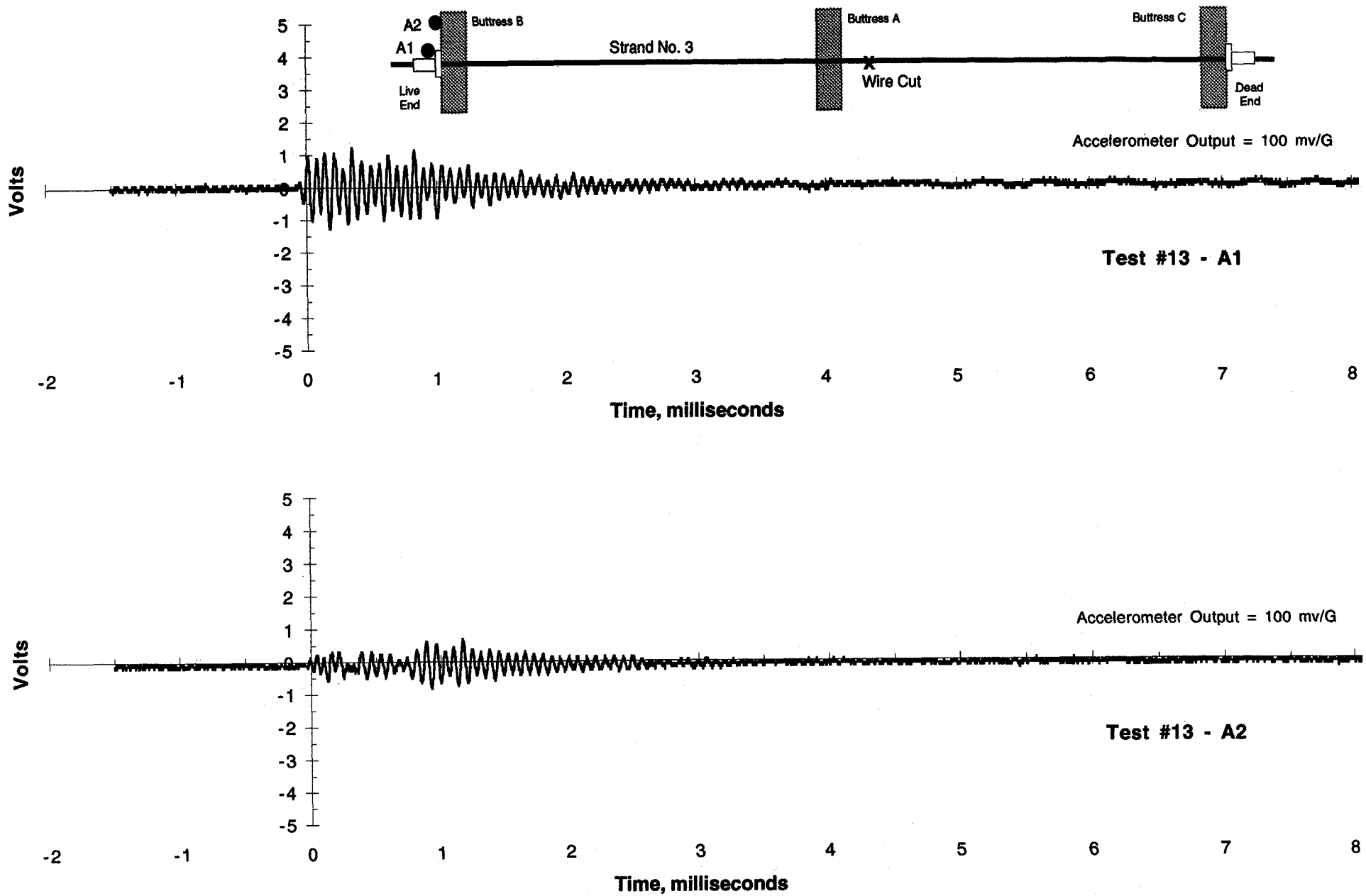

Figure 35. Time domain response of A1 and A2 in Test No. 13.

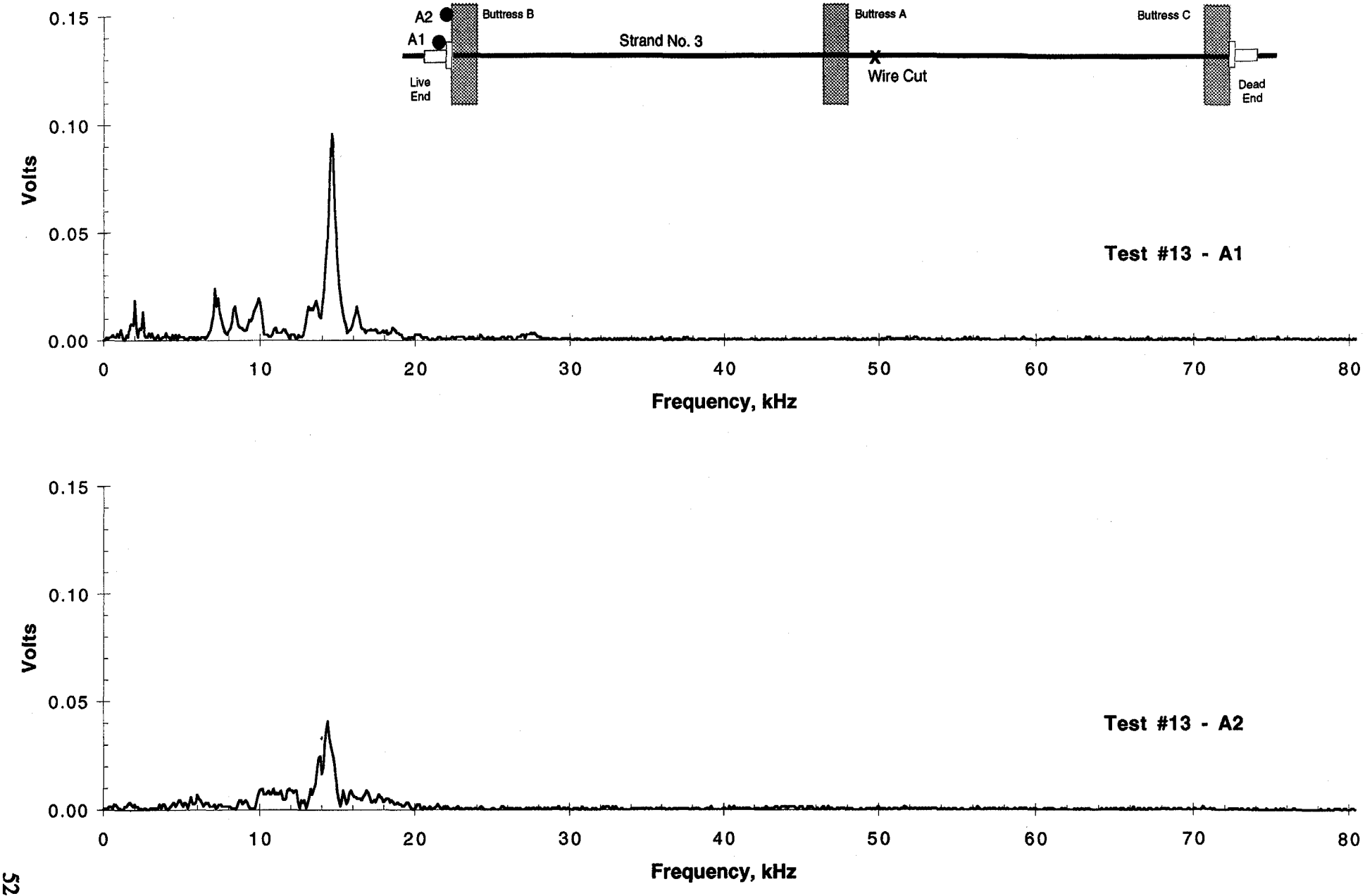

Figure 36. Frequency domain response of A1 and A2 in Test No. 13.

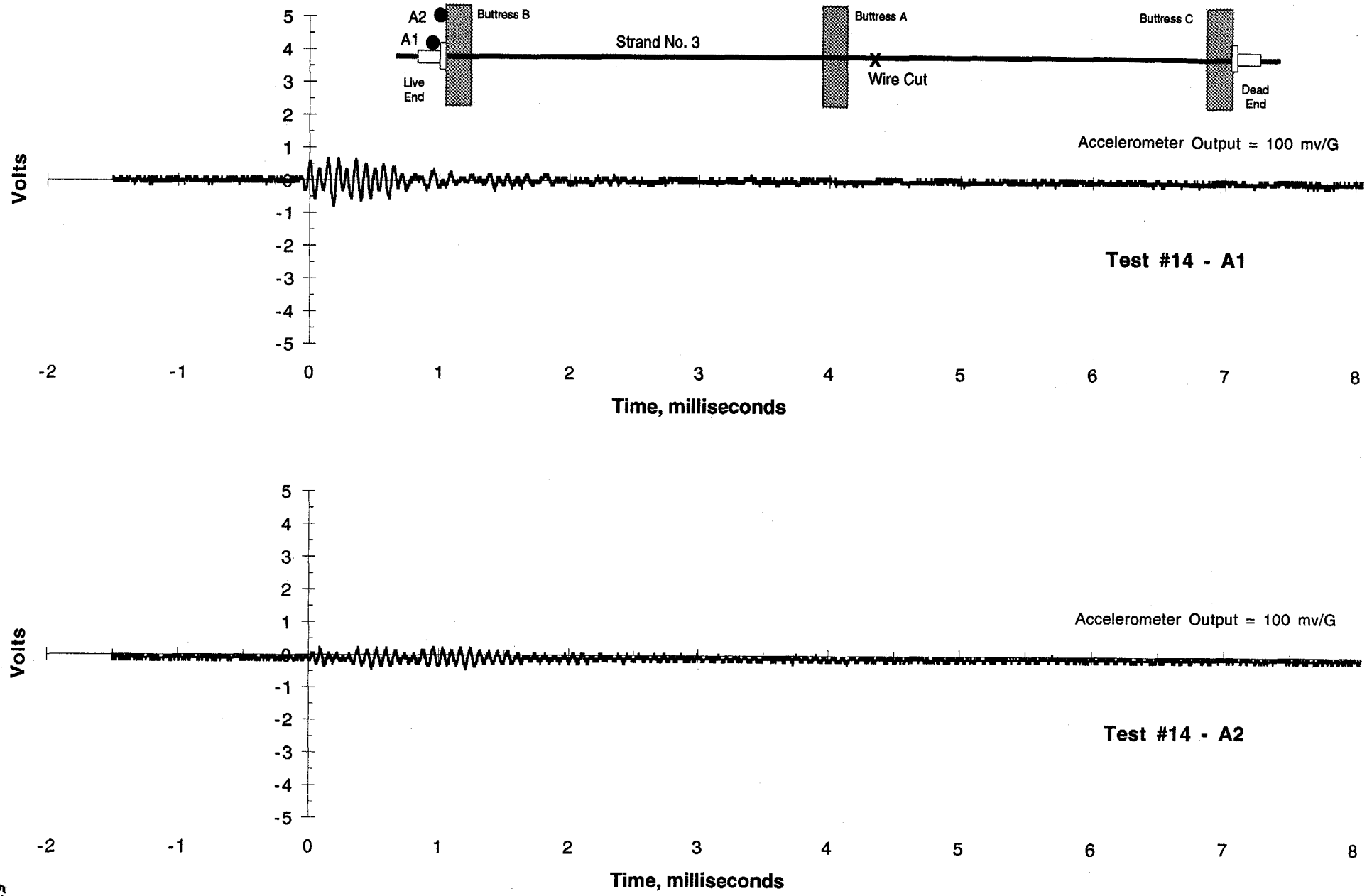

Figure 37. Time domain response of A1 and A2 in Test No. 14.

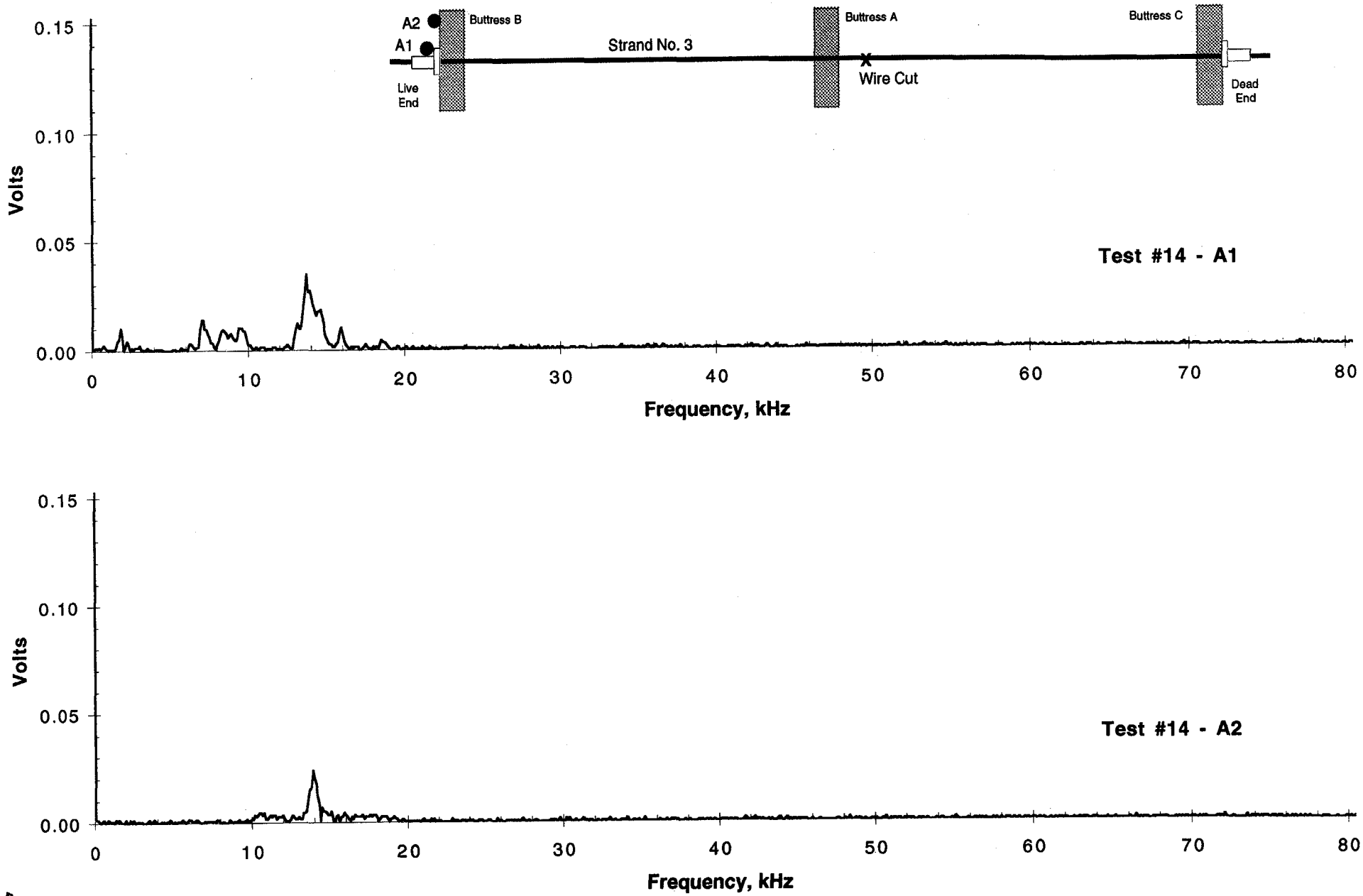

Figure 38. Frequency domain response of A1 and A2 in Test No. 14.

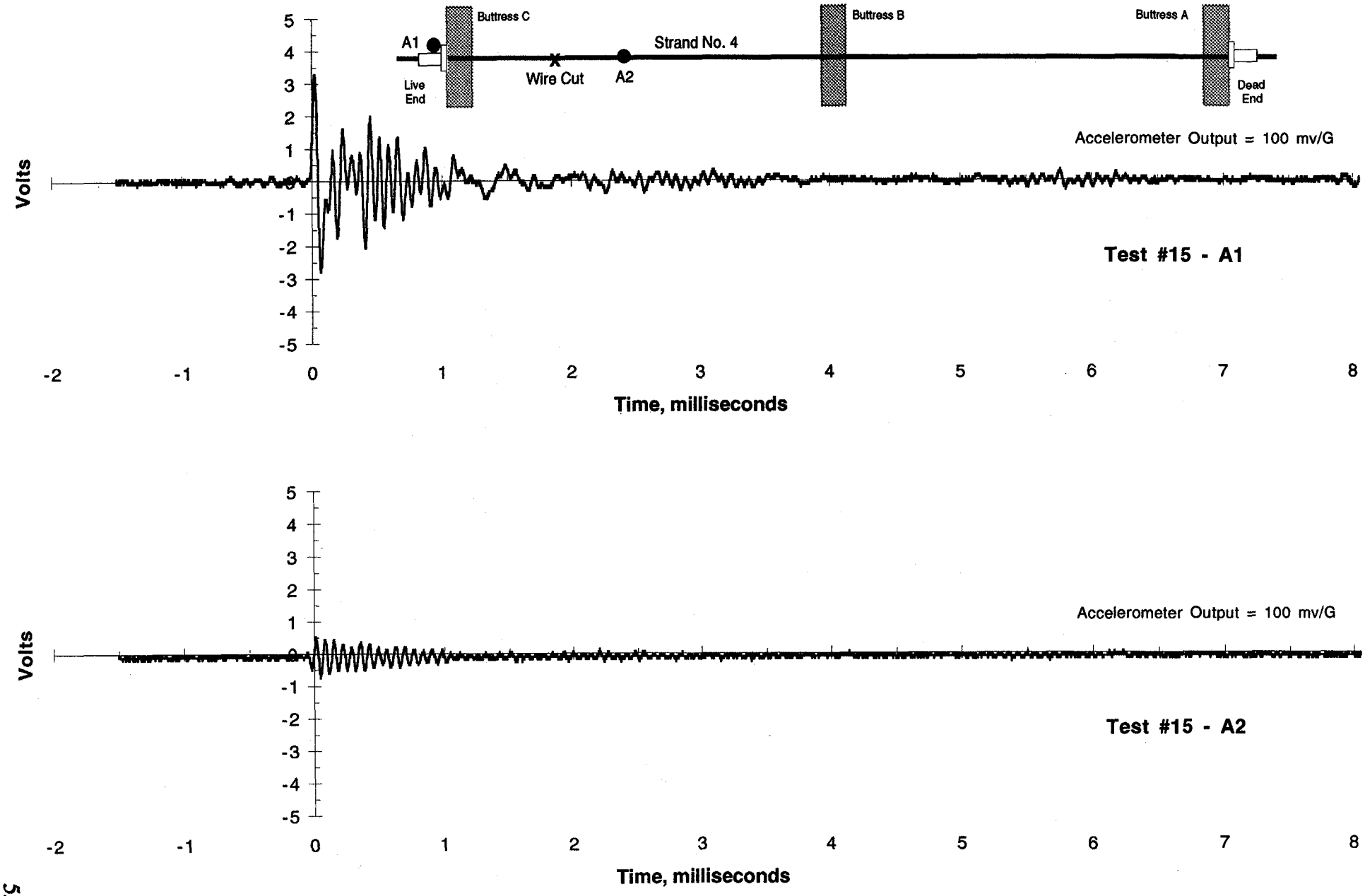

Figure 39. Time domain response of A1 and A2 in Test No. 15.

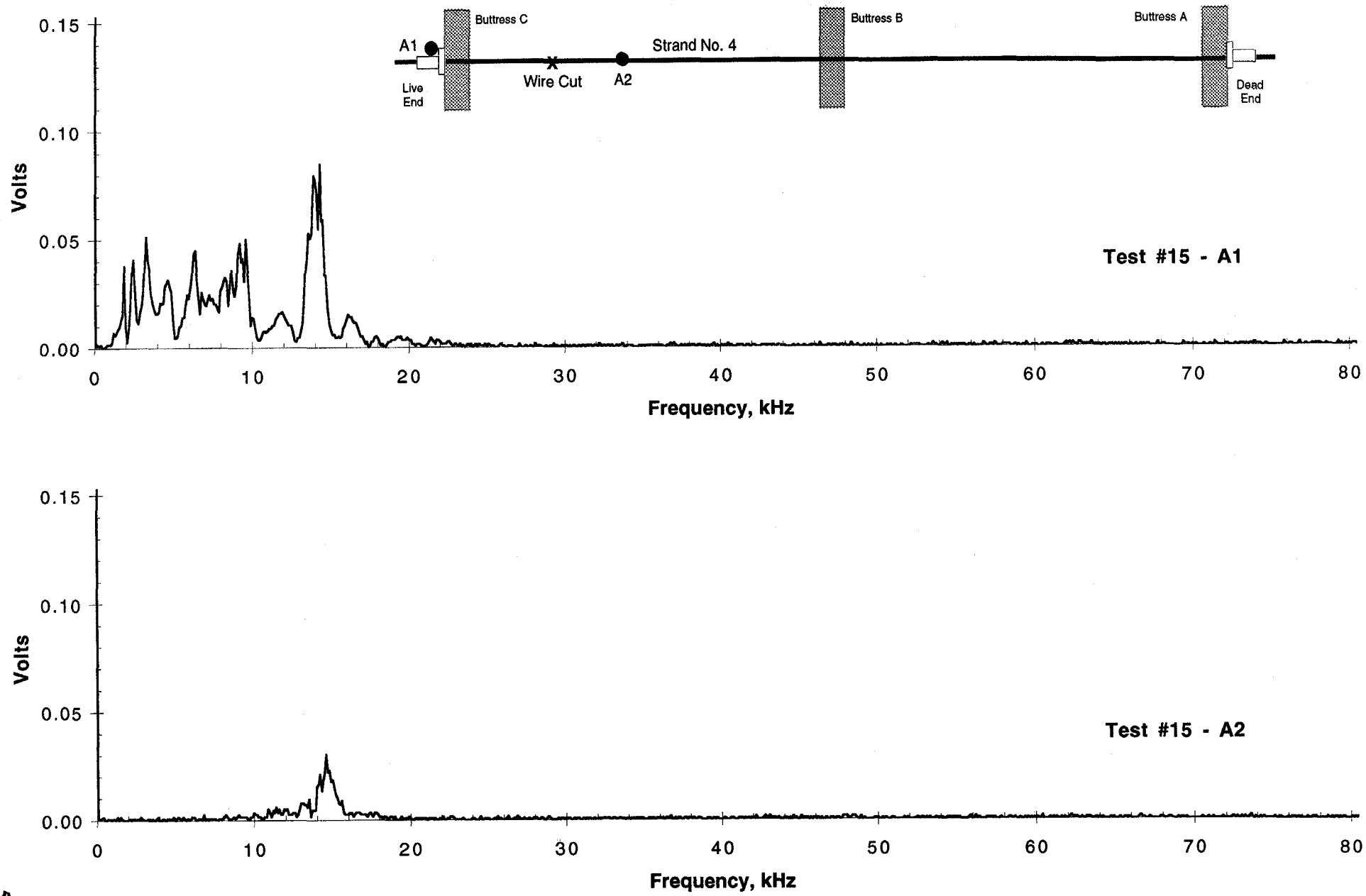

Figure 40. Frequency domain response of A1 and A2 in Test No. 15.

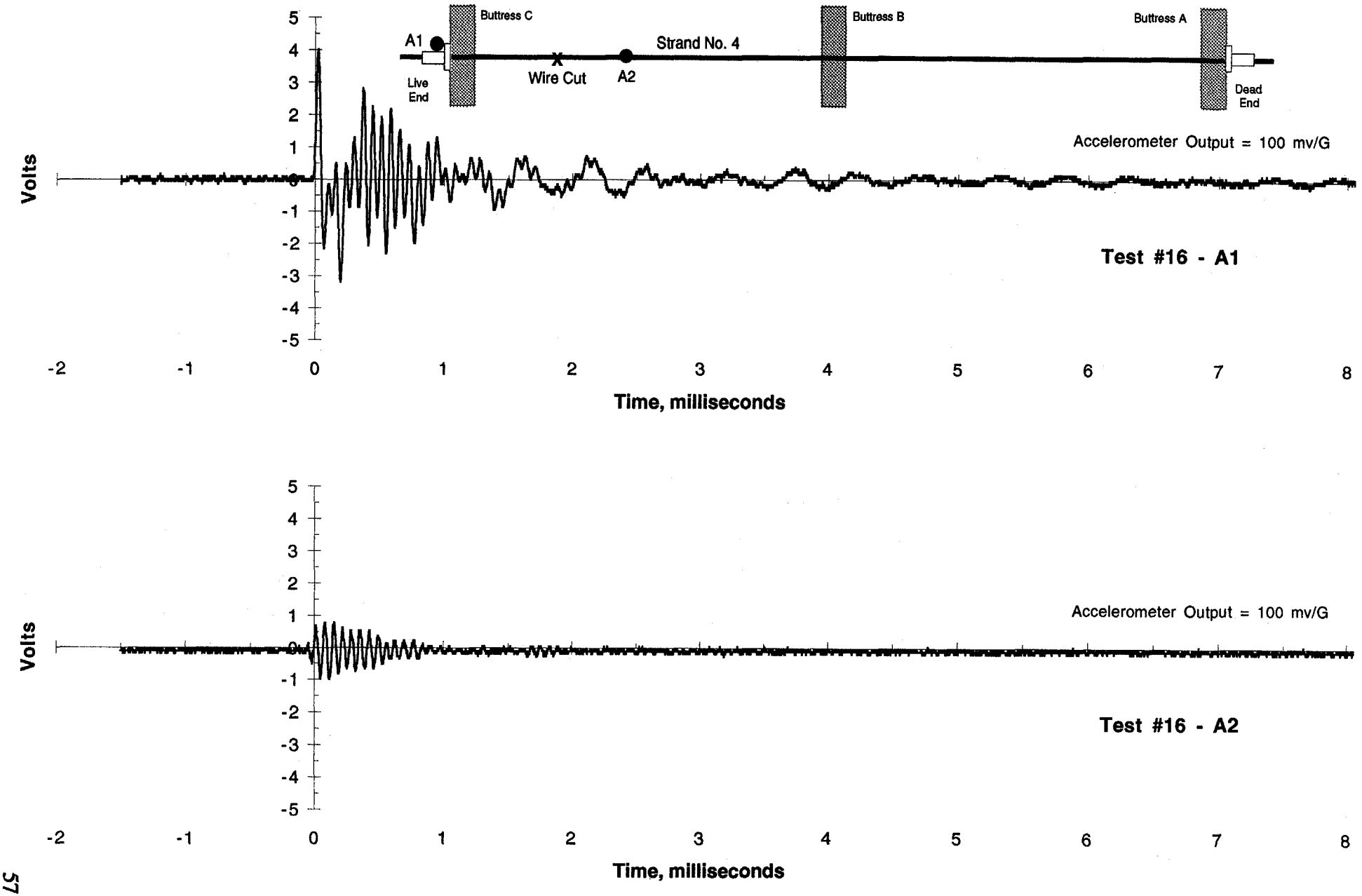

Figure 41. Time domain response of A1 and A2 in Test No. 16.

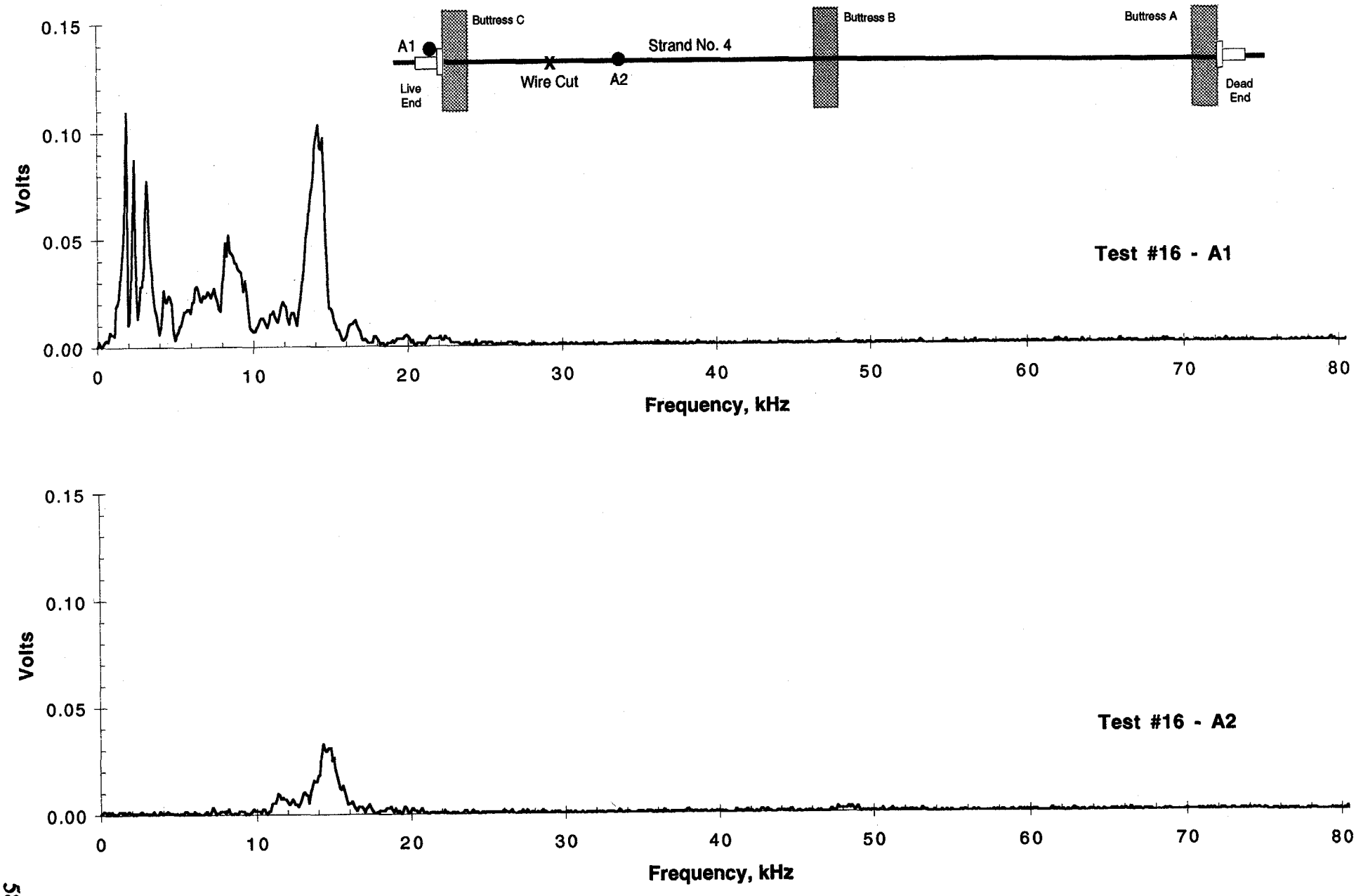

Figure 42. Frequency domain response of A1 and A2 in Test No. 16.

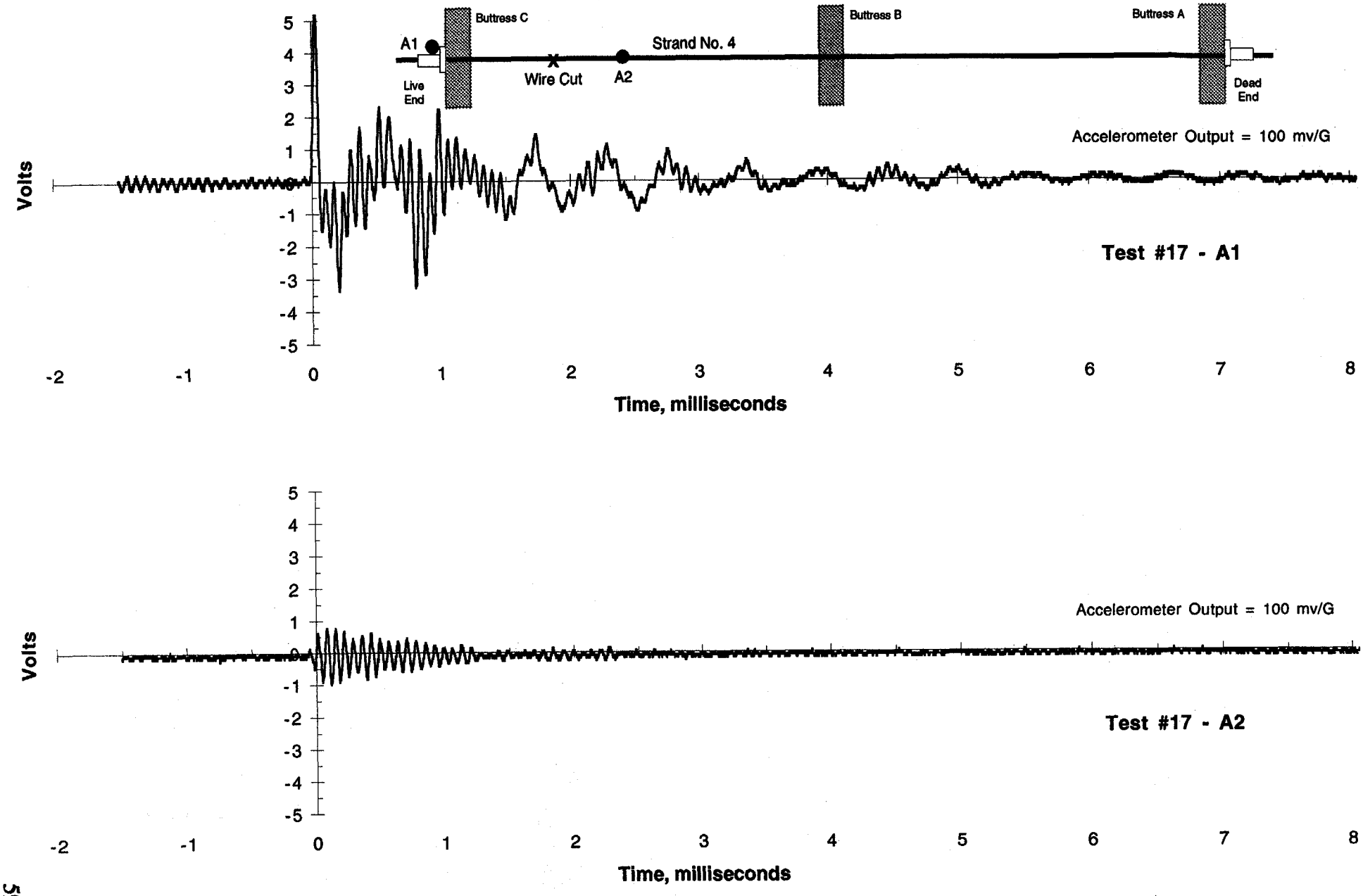

Figure 43. Time domain response of A1 and A2 in Test No. 17.

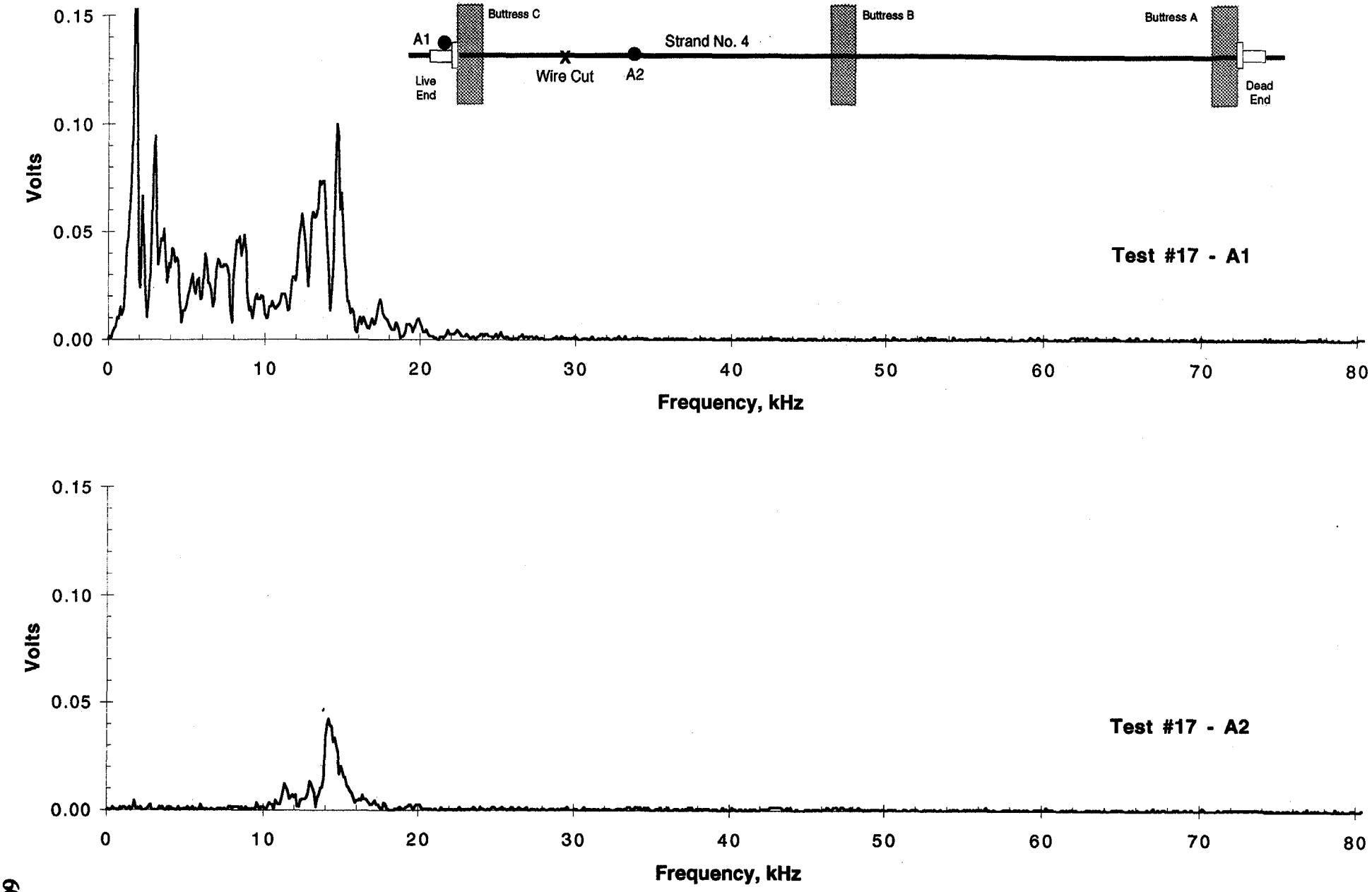

Figure 44. Frequency domain response of A1 and A2 in Test No. 17.

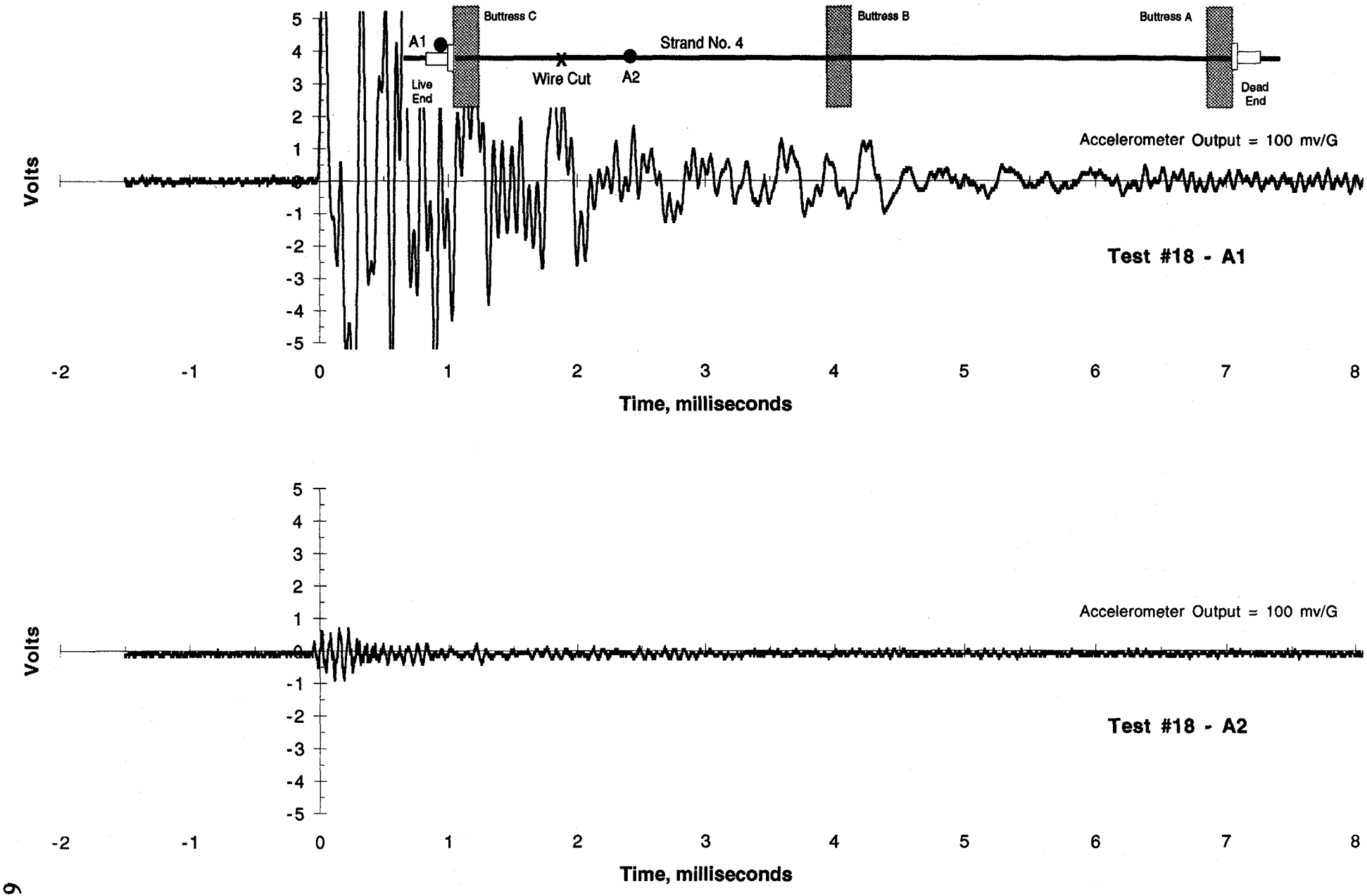

Figure 45. Time domain response of A1 and A2 in Test No. 18.

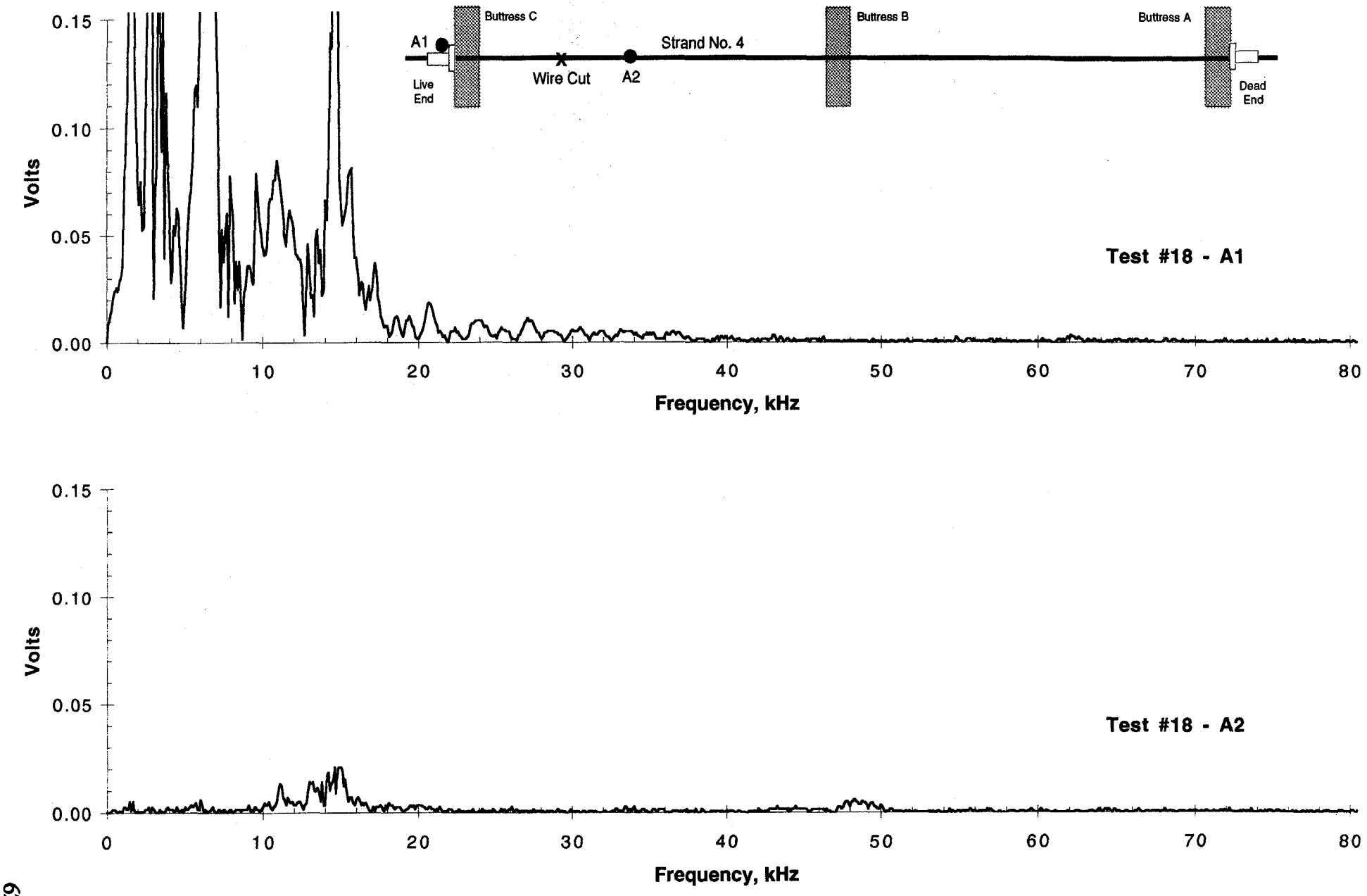

Figure 46. Frequency domain response of A1 and A2 in Test No. 18.

NRC FORM 335 (2-89) NRCM 1102, 3201, 3202

U.S. NUCLEAR REGULATORY COMMISSION

BIBLIOGRAPHIC DATA SHEET

(See instructions on the reverse)

1. REPORT NUMBER (Assigned by NRC, Add Vol., Supp., Rev., and Addendum Numbers, if any.)
NUREG/CR-6420

2. TITLE AND SUBTITLE
Self-Monitoring Surveillance System for Prestressing Tendons

3. DATE REPORT PUBLISHED
MONTH: December YEAR: 1995

4. FIN OR GRANT NUMBER
W6475

5. AUTHOR(S)
Habib Tabatabai

6. TYPE OF REPORT

7. PERIOD COVERED (Inclusive Dates)
May - Nov., 1995

8. PERFORMING ORGANIZATION – NAME AND ADDRESS (If NRC, provide Division, Office or Region, U.S. Nuclear Regulatory Commission, and mailing address; if contractor, provide name and mailing address.)
Construction Technology Laboratories, Inc.
5420 Old Orchard Road
Skokie, IL 60077

9. SPONSORING ORGANIZATION – NAME AND ADDRESS (If NRC, type "Same as above"; if contractor, provide NRC Division, Office or Region, U.S. Nuclear Regulatory Commission, and mailing address.)
Division of Engineering Technology
Office of Nuclear Regulatory Research
U.S. Nuclear Regulatory Commission
Washington, DC 20555–0001

10. SUPPLEMENTARY NOTES

11. ABSTRACT (200 words or less)

Assured safety and operational reliability of post-tensioned concrete components of nuclear power plants are of great importance to the public, electric utilities, and regulatory agencies. Prestressing tendons provide principal reinforcement for containment structures. In this phase of the research effort, the feasibility of developing a passive surveillance system for identification of ruptures in tendon wires was evaluated and verified. A one-tenth scale ring model of the Palo Verde nuclear containment structure was built inside the Structural Laboratory. Dynamic scaling (similitude) relationships were used to relate measured sensor responses (to intentional wire breaks) to the expected prototype response. Strong and recognizable signatures were detected by the accelerometers used. It is concluded that the unbonded prestressing tendons provide an excellent path for transmission of stress waves resulting from wire breaks.

Accelerometers placed on the bearing plates at the ends of tendons recorded high-intensity waveforms. However, accelerometers placed on concrete surfaces revealed substantial attenuation and reduced intensities. Locations of wire breaks were determined accurately through measurement of differences in arrival times of the signal at the two sensors. Pattern recognition systems utilized in conjunction with the proposed concept will provide a basis for an integrated and automated tool for identification of wire breaks.

12. KEY WORDS/DESCRIPTORS (List words or phrases that will assist researchers in locating the report.)
Prestressing
Tendon Surveillance
Wire Break Detection
Passive Monitoring System

13. AVAILABILITY STATEMENT
unlimited

14. SECURITY CLASSIFICATION
(This Page) unclassified
(This Report) unclassified

15. NUMBER OF PAGES

16. PRICE